AD-A148 981 AERODYNAMIC IMPROVEMENTS BY DISCRETE WING TIP JETS(U) 1/2
TENNESSEE UNIV SPACE INST TULLAHOMA GASDYNAMICS DIV
J M WU ET AL. MAR 84 AFWAL-TR-84-3009 F33615-81-K-3034

UNCLASSIFIED F/G 20/4 NL

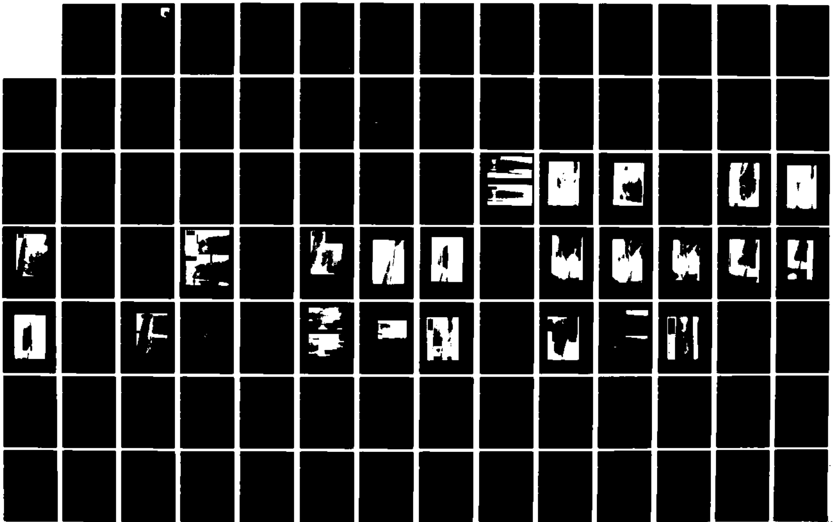

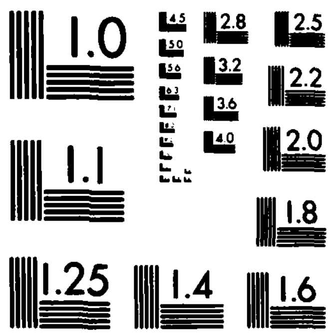

MICROCOPY RESOLUTION TEST CHART
NATIONAL BUREAU OF STANDARDS-1963-A

AFWAL-TR-84-3009

AERODYNAMIC IMPROVEMENTS BY DISCRETE WING TIP JETS

THE UNIVERSITY OF TENNESSEES SPACE INSTITUTE
GAS DYNAMICS DIVISION
TULLAHOMA, TENNESSEE 37388

MARCH, 1984

FINAL REPORT FOR PERIOD SEPTEMBER 1981 - NOVEMBER 1983

APPROVED FOR PUBLIC RELEASE; DISTRIBUTION UNLIMITED

FLIGHT DYNAMICS LABORATORY
AIR FORCE WRIGHT AERONAUTICAL LABORATORIES
AIR FORCE SYSTEMS COMMAND
WRIGHT-PATTERSON AIR FORCE BASE, OHIO 45433

NOTICE

When Government drawings, specifications, or other data are used for any purpose other than in connection with a definitely related Government procurement operation, the United States Government thereby incurs no responsibility nor any obligation whatsoever; and the fact that the government may have formulated, furnished, or in any way supplied the said drawings, specifications, or other data, is not to be regarded by implication or otherwise as in any manner licensing the holder or any other person or corporation, or conveying any rights or permission to manufacture use, or sell any patented invention that may in any way be related thereto.

This report has been reviewed by the Office of Public Affairs (ASD/PA) and is releasable to the National Technical Information Service (NTIS). At NTIS, it will be available to the general public, including foreign nations.

This technical report has been reviewed and is approved for publication.

WILLIAM D. FIELDS
Project Engineer

CHARLES J. COSENZA
Chief, Flight Vehicle Branch
Aeromechanics Division

FOR THE COMMANDER

RALPH W. HOLM
Colonel, USAF
Chief, Aeromechanics Division

"If your address has changed, if you wish to be removed from our mailing list, or if the addressee is no longer employed by your organization please notify AFWAL/FIM, W-PAFB, OH 45433 to help us maintain a current mailing list".

Copies of this report should not be returned unless return is required by security considerations, contractual obligations, or notice on a specific document.

UNCLASSIFIED

SECURITY CLASSIFICATION OF THIS PAGE (When Data Entered)

REPORT DOCUMENTATION PAGE		READ INSTRUCTIONS BEFORE COMPLETING FORM
1. REPORT NUMBER AFWAL-TR-84-3009	2. GOVT ACCESSION NO. AD-A148 987	3. RECIPIENT'S CATALOG NUMBER
4. TITLE (and Subtitle) AERODYNAMIC IMPROVEMENTS BY DISCRETE WING TIP JETS		5. TYPE OF REPORT & PERIOD COVERED Final Technical Report Sept. 81 - Nov. 83
		6. PERFORMING ORG. REPORT NUMBER
7. AUTHOR(s) J. M. Wu, A. D. Vakili		8. CONTRACT OR GRANT NUMBER(s) F33615-81-K-3034
9. PERFORMING ORGANIZATION NAME AND ADDRESS The University of Tennessee Space Institute, Gas Dynamics Division, Tullahoma, Tennessee 37388		10. PROGRAM ELEMENT, PROJECT, TASK AREA & WORK UNIT NUMBERS 2307N499
11. CONTROLLING OFFICE NAME AND ADDRESS Flight Dynamics Laboratory (AFWAL/FIMS), AF Wright Aeronautical Laboratories (AFSC), WPAFB, OH 45433		12. REPORT DATE March 1984
		13. NUMBER OF PAGES 94
14. MONITORING AGENCY NAME & ADDRESS(if different from Controlling Office)		15. SECURITY CLASS. (of this report) Unclassified
		15a. DECLASSIFICATION DOWNGRADING SCHEDULE

16. DISTRIBUTION STATEMENT (of this Report)

Approved for public release, distribution unlimited.

Accession For	
NTIS GRA&I	X
DTIC TAB	☐
Unannounced	☐
~~Justification~~	
By	
Distribution/	
Availability Codes	
Dist	Avail and/or Special
A-1	

17. DISTRIBUTION STATEMENT (of the abstract entered in Block 20, if different from Report)

18. SUPPLEMENTARY NOTES

DTIC COPY INSPECTED

19. KEY WORDS (Continue on reverse side if necessary and identify by block number)

Discrete Jets
Tip Blowing
Vortex Control
Wing Tip Jets
Jet Vortices
Flow Visualizations
Water Tunnel Tests

20. ABSTRACT (Continue on reverse side if necessary and identify by block number)

The effects of applying discrete wing tip jets on a rectangular wing and the generated flow field have been studied. Analysis included low speed wing tunnel testing, water tunnel testing and analytical modeling. Wing tip jet parameters investigated included number of jets, jet direction, shape of jets, and blowing coefficients. Tailoring of jet parameters to optimize planform circulation and flow separation were included. Flow interactions of the discrete tip jets with wing vorticies were successfully visualized with water tunnel techniques.

DD FORM 1 JAN 73 1473 EDITION OF 1 NOV 65 IS OBSOLETE

UNCLASSIFIED

SECURITY CLASSIFICATION OF THIS PAGE (When Data Entered)

SUMMARY

The effects of applying discrete wingtip jets on a rectangular wing and the generated flow field have been studied. Quantitative measurements were made in a low speed wind tunnel. Surface pressure measurements indicated significant improvements on the wing lift with the discrete jets blowing. The jet blowing coefficient range, C_μ was in the order of 0.001 to 0.01. It was observed that even with such small jet blowing, the entire wing circulation has been altered. The entire chordwise and the spanwise surface pressure distributions were perturbed by the jet effect. This is attributed to the local flow interactions which enhanced the total wing circulation. Detailed flow field observations of interactions between the wingtip jets and the flow around the wingtip were made in a water tunnel. Higher jet coefficients in the water tunnel study were used for enhancement of the observations. Complex flow interaction phenomena were observed with the jets blowing. Several types of peculiarly behaving secondary and auxiliary vortices were observed. Some vortices spun around axes perpendicular to the main tip vortex core and were periodic. Other vortices observed rotating in opposite sense with their axes nearly parallel to the tip vortex. Such secondary vortices have significant influence on the tip wake flow. In general, the wing tip flow field was favorably affected by the discrete jets and significant dispersion of the tip vortex was observed. Two analytical models have been considered for the comparison with the wind tunnel data and water tunnel observations. The present study indicates that the wingtip jets, if applied properly, could be developed as a viable means for improving and controlling the wingtip flow field.

TABLE OF CONTENTS

LIST OF ILLUSTRATIONS

1. INTRODUCTION AND TECHNICAL BACKGROUND

The tip region of a lifting wing contains a complex three-dimensional viscous flow field resulted from unequal pressure distributions on the upper and lower surfaces of the wing. The details of the flow in the tip region can have a major effect on the performance of a wing. This complicated flow at the tip region of a wing varies significantly with the geometry of the wing tip. If the wing produces lift but has zero circulation at the tips, vorticity must be shed. The shed vorticity creates the trailing vortex system which is responsible for downwash and induced drag.

Ever since it was recognized that the three-dimensional wing produced an *induced drag*, many efforts have been made to reduce the induced drag and to increase the overall lift/drag ratio by properly modifying the wing configuration including its tips. It is astonishing to learn that as early as 1897, a patent was issued to Lanchester for installing a vertical plate at the wing tips (Reference 1). The search for better means of reducing the induced drag has never ceased. Indeed it has a long history, almost as long as the history of aviation itself.

Among numerous works done on this subject, a few significant decisive milestones were established by Munk (Reference 2) in 1921, Reid (Reference 3) in 1925, Hemke (Reference 4) in 1927, Von Karman and Burgers (Reference 5) in 1934, Mangler (References 6 and 7) in 1937 and 1939 of early theoretical methods, Reiba and Watson (Reference 8) in 1950, Riley (Reference 9) in 1951, Clements (Reference 10) in 1955 all contributed in early experimental observations. Later, Weber (Ref-

erence 11) in 1956, Cone (Reference 12) in 1962, Lundry and Lissaman (Reference 13) in 1968 all contributed in further developments of the wing-tip end-plate theory.

In 1976, Whitcomb (Reference 14) summarized all of the end plate ideas and proposed to install a small half-wing (called winglet) on the wingtip in order to improve the local wingtip surface pressure distributions. This winglet modification of wingtip has proven to be effective (Reference 15) if designed properly.

The end-plates as well as winglets are all fixed solid bodies which lack flexibility suitable for the various phases of flight. To overcome this inherent disadvantage, a new concept has been conceived to place several small jets at the wingtip (Figure 1). If these jets produce a similar favorable change in the flow field, it will have a definite advantage over end-plate at the wingtips. The wingtip jets can be implemented with sufficient flexibility and also can be turned on or off according to various flight conditions. After the idea was conceived, a preliminary experimental study was conducted using a basic wing model in a low speed wind tunnel. The preliminary results have been published in References 16 and 17.

After the publications of our preliminary results on the wind tunnel experiments (Reference 16), we learned of the studies made by Lloyd (Reference 18) and Carafoli and Camarasescu (Reference 19). In both of these studies massive spanwise jet blowing was used to increase the apparent aspect ratio of a wing. The jet was blown from a single long slit along the entire chord length at the wingtip of a low aspect ratio wing. This is in contrast to our idea of trying to utilize favorably the

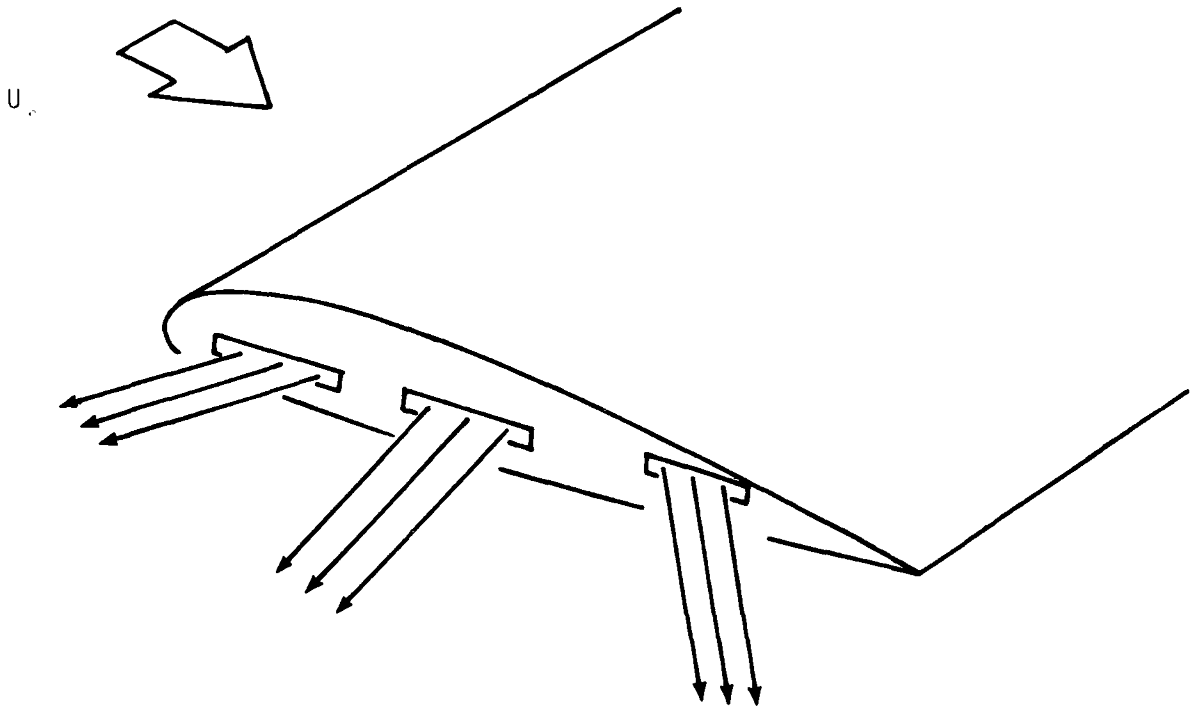

Figure 1. Concept of Individually Controlled Discrete Wing Tip Jets

local flow interactions. Consequently their jet coefficient was one to two orders of magnitude higher than in the current experiments.

Recently Briggs and Schwind (Reference 20) investigated the use of a wingtip jet sheet to reduce takeoff and landing distances of advanced fighter aircrafts. Again, their jets were relatively massive in comparison to ours. They studied the effects of wing taper ratio and the jet shape. Narrow jet slits were found less effective in increasing lift at jet blowing coefficients C_μ less than 0.1 than were thicker jets, where jet thickness varied proportional to the wingtip thickness. Higher jet coefficients of the thin jets were found to be more effective than the thicker ones. Our literature survey indicated that the most successful wingtip jet blowing study was conducted by Yuan and Bloom (Reference 21). They mounted a circular tube extended in the spanwise direction from the trailing edge of the wingtip. The jets were blown downward. With relatively small jet blowing coefficient, they achieved a remarkable improvment on the wing performance. However, without further detail study to understand the flow phenomena, they immediately tried to apply it to a larger aircraft's wing configuration. As a consequence it did not obtain the expected result and therefore, the study was abandoned. A case of prematurely rushing a preliminary research result into real configuration hardware applications.

The discrete wingtip jet concept originated as a means to provide wing tip flow field control beyond what can be achieved by winglet type modifications. This additional measure of control results from two influences (Figure 2). First, the discrete jets can be independently controlled with respect to direction and amount of blowing. This enables

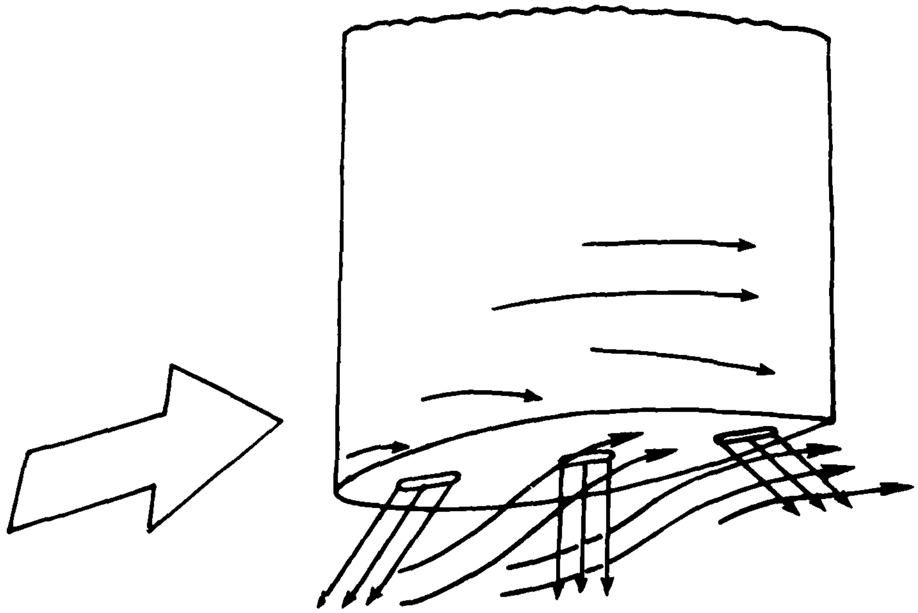

(a) Schematic of Individually Controlled Jet and Flow Interaction

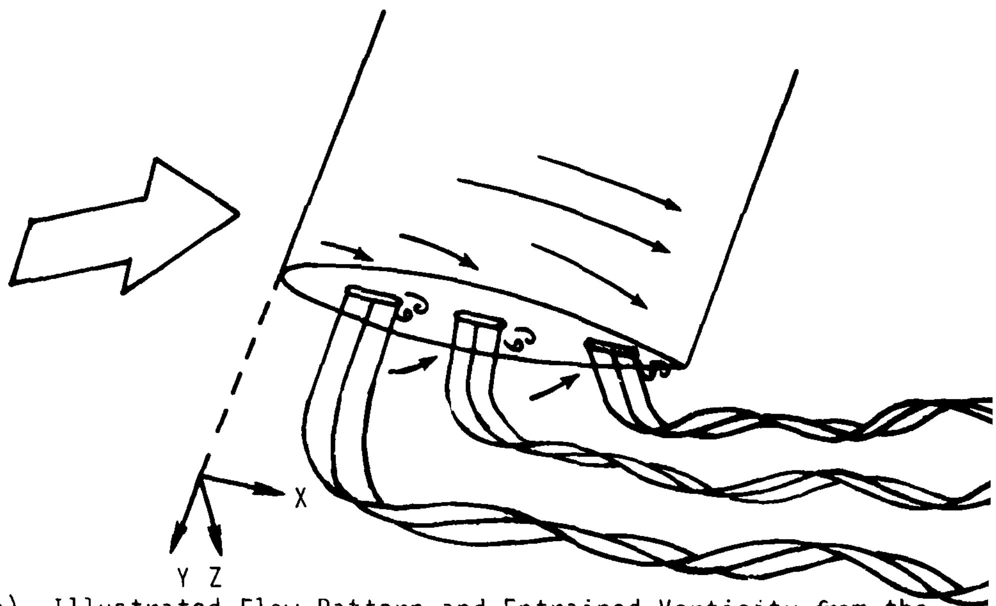

(b) Illustrated Flow Pattern and Entrained Vorticity from the Wing Surface

Figure 2. Discrete Wingtip Jet Induced Flow Interactions and Coor

each jet to be designed such that it creates the desired flow characteristics in the region of the flow field where its influence is the strongest. The second influence providing additional control is the proper utilization of local flow interactions. The occurrence of the counter rotating vortex pair is characteristic of a jet in cross flow. It was expected that these vortices interacting with the wing tip flow field would produce desired modifications resulting in improved performance of the wing and reduction of the induced drag.

Our water tunnel flow visualization experiments have confirmed that the discrete jets in the local wingtip cross flow could produce many complicated auxiliary and secondary vortices. The production of auxiliary vortices and their interaction with the main vortex system can also be an effective measure in alleviating wake vorticity. The secondary vortices draw a portion of their energy from the wingtip vortex and consequently reduce its strength. This process also creates more interaction in the wake region and thus hasten the decay of the entire vorticity. These influences should be beneficial in decreasing the downwash as well as in reducing the wake hazard.

The auxiliary vortices are important contributors to the accelerated spreading of vorticity into the wake surroundings. This can be shown directly by examining the Helmholtz equation for the time rate of change of vorticity. The $(\vec{\omega} \cdot \nabla)\, \vec{u}$, so called vortex stretching term, in the Helmholtz equation is zero for two-dimensional flow, and thus vortex spreading is simply a viscous diffusion process. This term is nonzero when a component of vorticity is aligned with a velocity gradient. In the typical wake vortex the strongest component of the vorticity

vector, by far, is the x -direction component which is aligned with the free stream. Unfortunately the velocity gradient in the x-direction is quite small and $(\vec{\omega} \cdot \nabla)\,\vec{u}$ is still a weak contributor to vorticity spreading. However, the contribution of this term is greatly increased by the production of secondary vortices such as were seen in our preliminary water tunnel experiments. These vortices were originally aligned with the radial direction and their contribution to the $(\vec{\omega} \cdot \nabla)\vec{u}$ term is $\omega_r \frac{\partial u}{\partial r}$. Of course $\frac{\partial u}{\partial r}$ is typically quite large in the vortex, larger than the velocity gradient in any direction. Thus, $\omega_r \frac{\partial u}{\partial r}$ will greatly increase the magnitude of $(\vec{\omega} \cdot \nabla)\vec{u}$ and consequently the rate at which vorticity is spread. It is for these reasons that secondary vortices are considered relevant in producing accelerated vortex decay and will alter the initial formation of the tip vortex flow in the vicinity of the wing tip.

Finally, the discrete wingtip jet will generate considerable turbulence in the wake roll up region. While not a flow control mechanism, nevertheless, controlled disturbing flow is beneficial in accelerating vortex decay downstream through either Crow instabilities or viscous diffusion (Reference 22 and 23).

It is expected that discrete jets can also support a pressure difference in a similar manner to jet sheets at the wing tip. This would also result in reduced downwash and reduced induced drag due to the effective increase in aspect ratio. Hopefully the discrete jets can be optimized such that induced drag reductions, comparable to those supplied by the jet sheet, can be achieved at lower jet coefficients.

In addition to conventional airplane wings, discrete wing tip jets could also be applied on rotary wing aircraft. Alleviation of tip vortices

is an important goal in that situation due to the vortex impingement or blade-slap problem.

2. WIND TUNNEL EXPERIMENTS AND RESULTS

The principal measurements conducted in the wind tunnel experiments were the surface pressure distributions on the wing. The force and moment measurements were not successful due to the air supply tubes interfering with the balance.

Description of Facility and Models

All of the wind tunnel experiments were performed in the University of Tennessee Space Institute (UTSI) low speed wind tunnel. This facility is an open circuit, closed test section, continuous wind tunnel. The test section measured 35.6 cm × 50.1 cm × 107 cm (14 in. × 20 in. × 42 in.) height, width and length respectively. The plexiglass side-wall allows observation and photography of the model. The tunnel velocities range from 6.1 to 30.5m/sec (20 to 100 ft/sec). Pressure measurements are made with ± 1 psid transducers which are used with two twenty-four port wafer switches. Data acquisition is managed by a minicomputer specially designed for this purpose. Almost all of the tests were performed at 20m/sec (65 ft/sec) tunnel speed, with unit Reynolds number of 0.4×10^6.

The model used for these test was a NACA0012-64 airfoil with 18.00 cm chord length and 30.48 cm half span. The model was made from many modular pieces so that access to the inside, for the purpose of instrumentation as well as air supply to the wingtip jets, was readily possible. Pressure ports were provided at four span stations. There were nine pressure ports on the upper surface and seven ports

on the lower surface for each row. The model was supported by a sting through the tunnel side wall to a machinist turntable with the capacity of continuous incident angles setting of 0^0 to 360^0. A boundary layer fence was installed between the model and tunnel wall to ensure local two dimensional flow. Figure 3 shows the wind tunnel experimental set up.

The model was equipped with interchangable tips and these tips were designed to provide various combined blowing configurations. The data presented here were taken with different wingtip jets shown in Figure 4. Blowing air was supplied to the individual tip jets through 0.64 cm diameter tubing and the flow rate was measured in each tube. Total pressure in the air supply line was varied to obtain different jet blowing rates.

Force and moment measurements were made using a small (1.27 cm diameter) six component sting-balance. The model was mounted on the balance with the sting passing through its maximum thickness location, as shown in Figure 3. Individual air supply tubings were routed around the sting through the model opening and connected to the tip jets. The tubes were installed only when blowing was employed. otherwise they were removed. The force and moment measurements made with wingtip jets blowing proved to include interferences caused by the air supply tubings. This interference could not be isolated or resolved without redesigning the entire experimental arrangement. However, the baseline normal force measurements agreed with the value obtained by the integration of pressure data.

The maximum blockage of the model at $\alpha = 10^0$ in the tunnel was

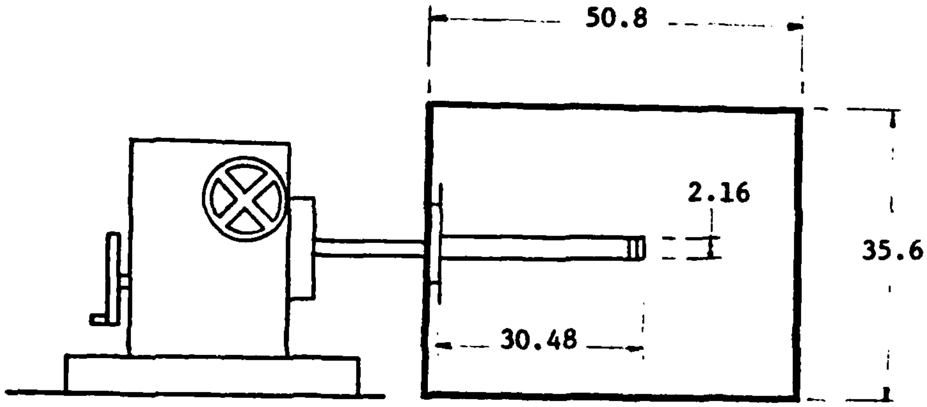

Dimensions in centimeters

(a) Schematic of Sting Mounted Half-Wing Model

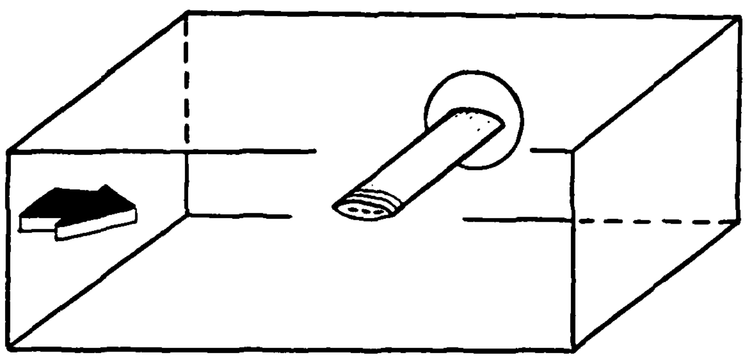

(b) Pictorial View of Test Section

Figure 3. Experimental Set-up in the Wind Tunnel

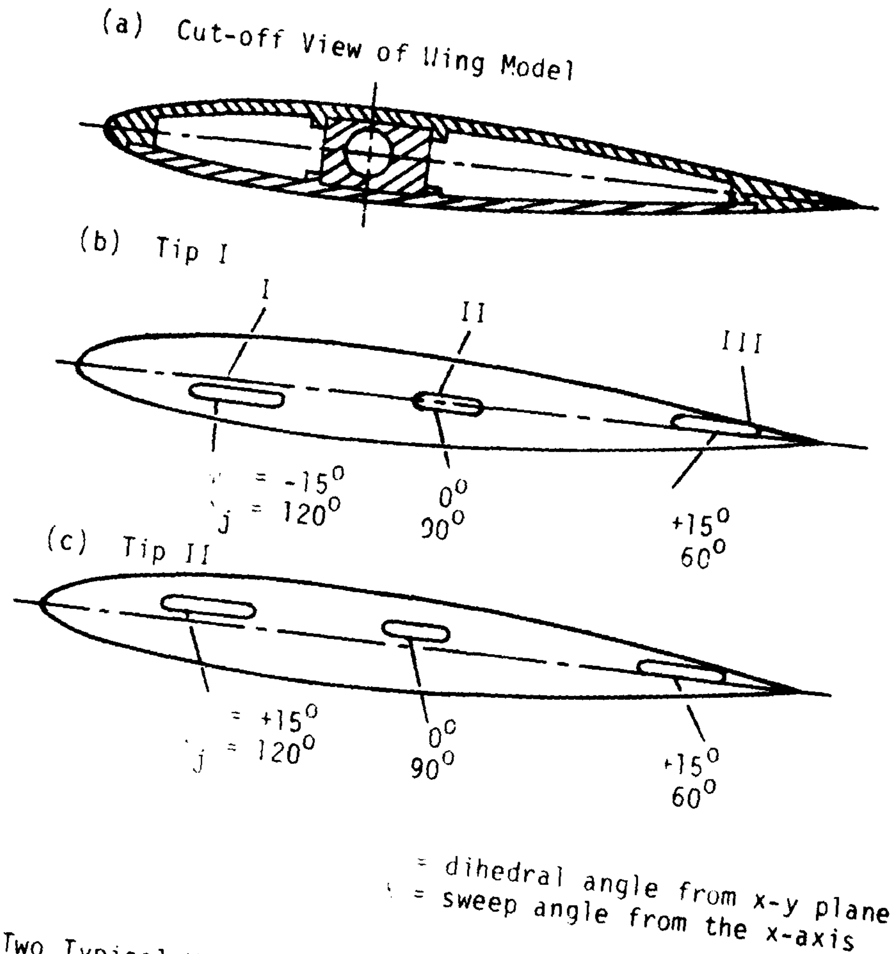

Figure 4. Two Typical Wing Tip Jet Ports Configurations.

5.3% in this study. The presence of wind tunnel walls often introduce tunnel interferences which does not exist in free flight testings. Depending on the model geometry and size in relation to the wind tunnel test section, corrections can be applied to the wind tunnel data. Two basic approaches for prediction of the tunnel interferences are: (1) the image and vortex lattice method; (2) measured wall pressure distribution. The first method has been used in this investigation. Following Pope, corrections to the angle of incidence due to the tunnel wall effects can be written as:

$$\Delta\alpha = \delta \frac{S}{C} C_L 57.3$$

where: δ is the boundary correction factor, S is the wing area, C is the tunnel cross section area, C_L is the lift coefficient.

Wind Tunnel Results

In the absence of a fundamental theoretical understanding of the wingtip jet flow field interactions, this experimental study was based on a systematic parametric investigation. Baseline measurements (with no wingtip jets) of pressures at three spanwise stations and force and moments using the six component balance were carefully made to be used as a reference for comparison with the data gathered with various wingtip blowing configurations. As noted earlier, force and moments measurements using the six component sting mounted balance was found to have interference due to air supply tubings. This problem could only be resolved by redesigning the experimental set-up, which was found to be excessive for the present study, however, will be consid-

ered in the design of future investigations. The measurements made by the balance indicated, due to tube interference, the net improvements in lift and drag were not comparable with the integrated pressure measurements. But the baseline measurements of the balance measured normal force and the pressure data agreed well. Therefore, pressure measurements integrated over the model have been used to obtain normal force coefficients with various jet blowing configurations.

The baseline pressure distribution indicated the variation in the loading along the half-wing span as shown in Figure 5. Wingtip blowing produced increased lift over the entire model. A typical variation in the pressure distributions on the upper and lower surface of wing with and without jet blowing is shown in Figure 6. For some jet arrangement no improvment was observed, only certain configurations of blowing resulted in improved C_p distribution. This implies that orientation and location of the jets are important and critical. A careful study is a must before any attempt for the actual application, in order to achieve the maximum benefit.

Overall Circulation Change with Jets

It is interesting to note that improvements in the pressure distribution is fundamentally different than that of the winglet. The winglet application utilizes the principle of pressure superposition and its effect is very much localized. In contrast, pressure improvement over the entire chord as well as span were observed due to the discrete jet blowing. In the present case a more *global* improvement was obtained. This implies that the basic *wing circulation* and the *bound vortex* were

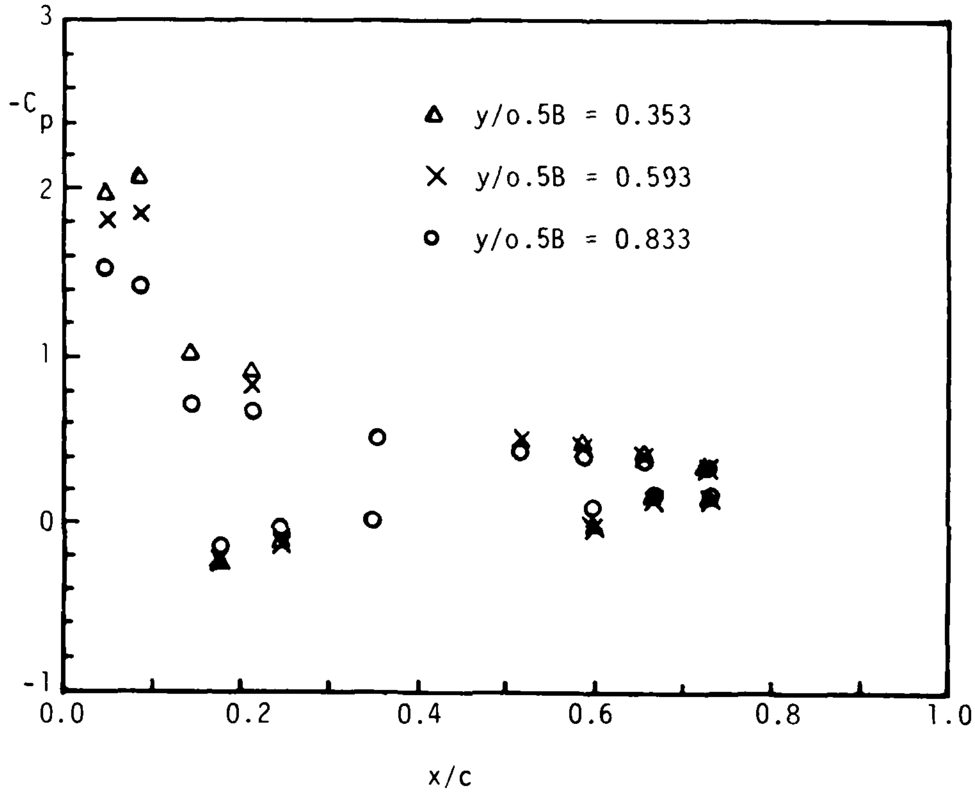

Figure 5. Pressure distribution on the wing for Alpha=10^0, no blowing.

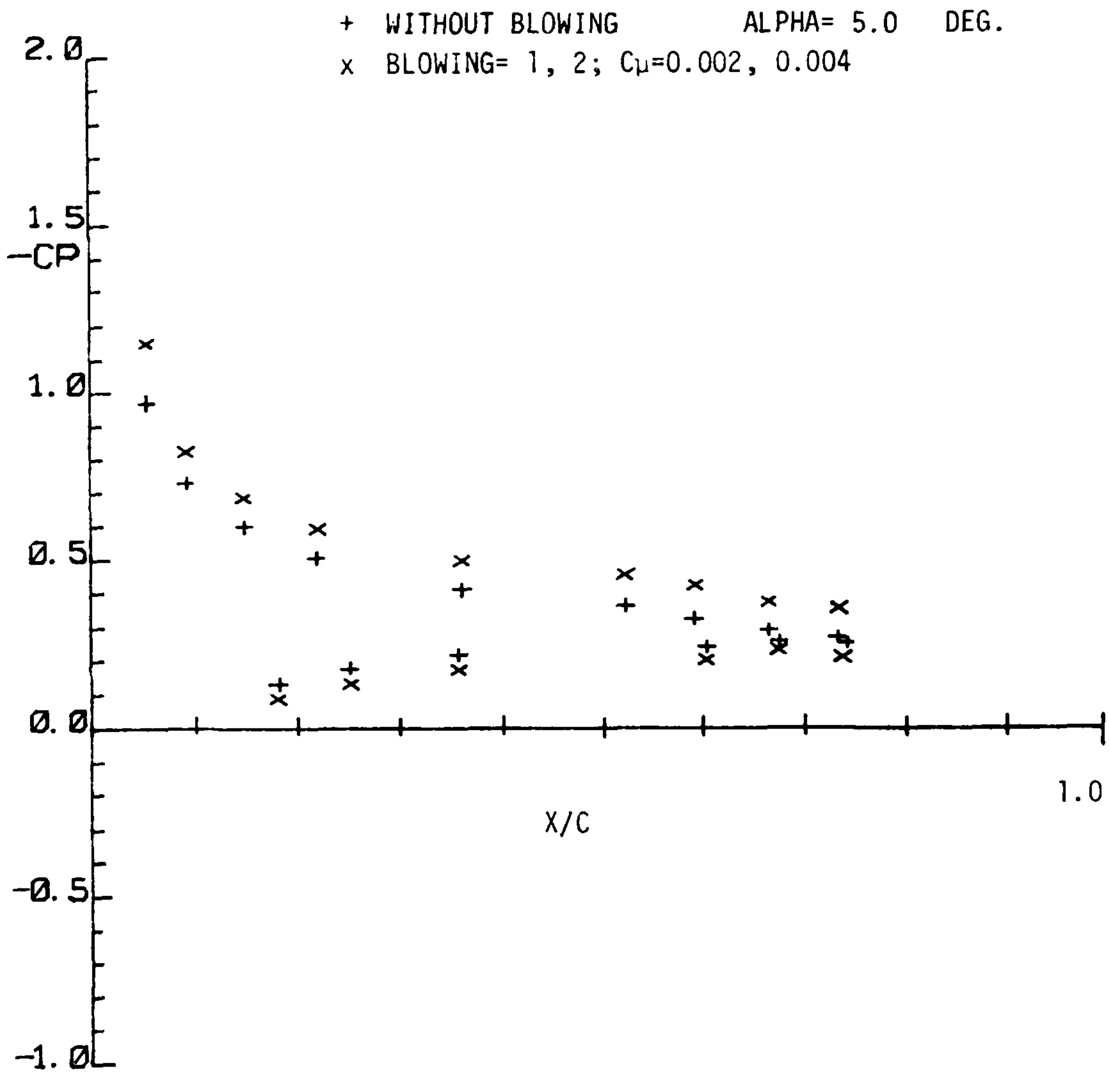

Figure 6. C_p Distribution on the Wing at y/0.5B = 0.833 (Near Tip); Typical.

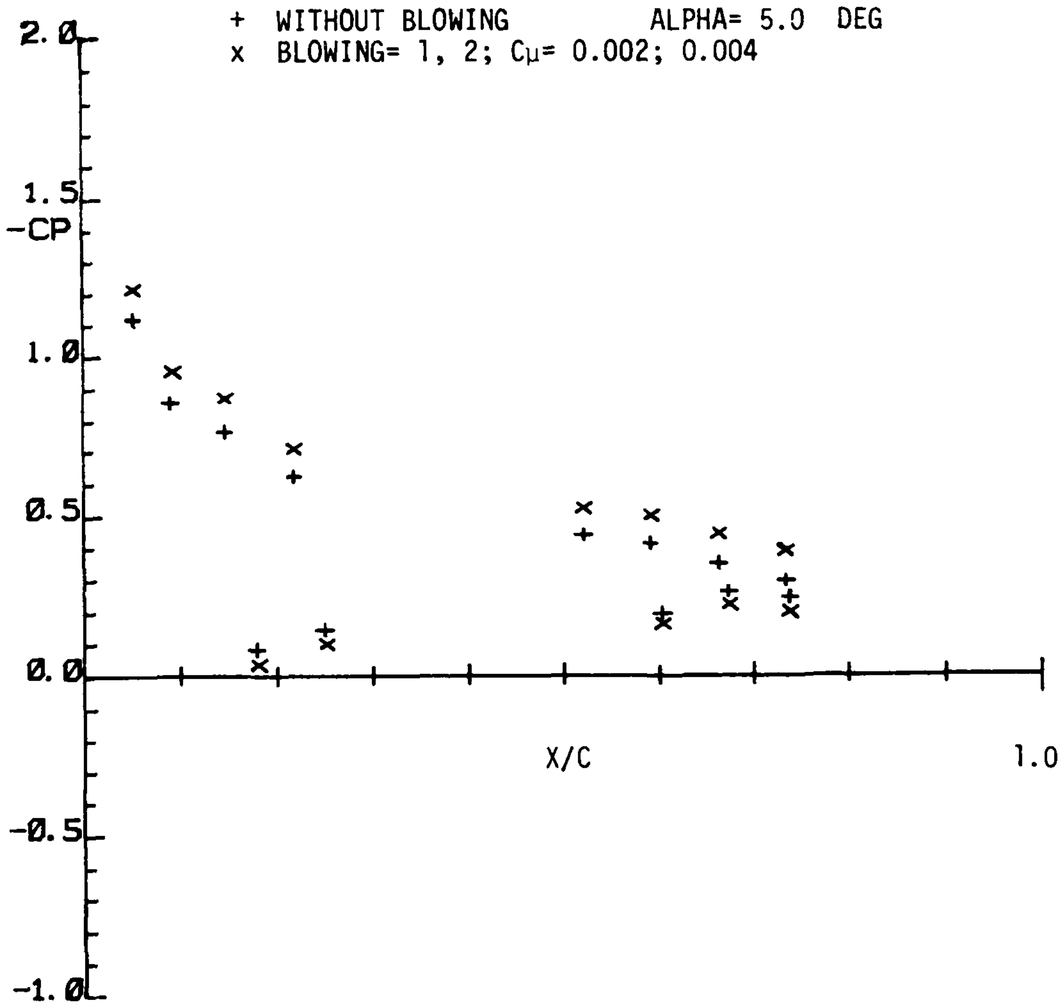

Figure 6 (Continued) C_p Distribution on the Wing at y/0.5B = 0.593

(Near Quarter Span) Typical.

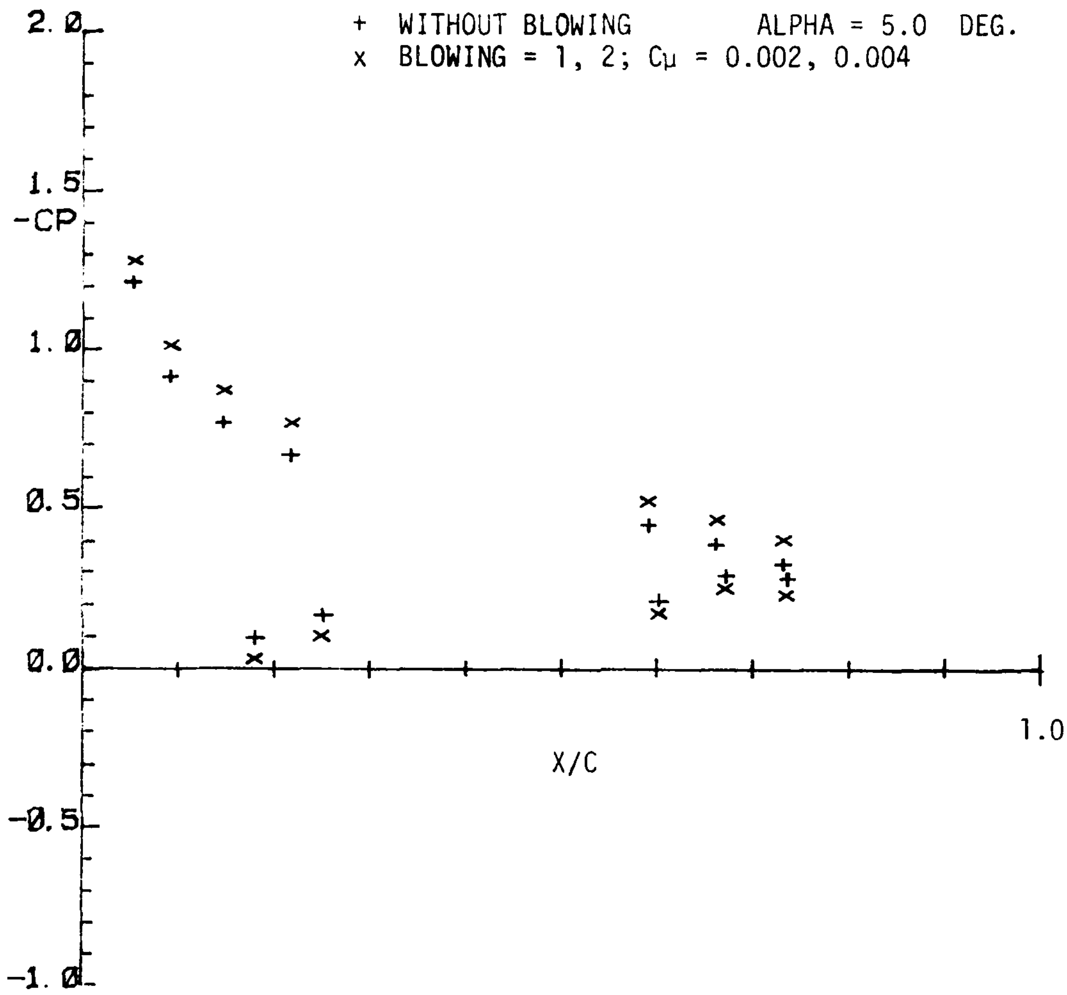

Figure 6 (Continued) C_p Distribution on the Wing at y/0.5B = 0.353 (Near Root) Typical.

changed because of jet blowing. The normal force coefficien
the incidence angles for a few typical tip configurations is
Figure 7.

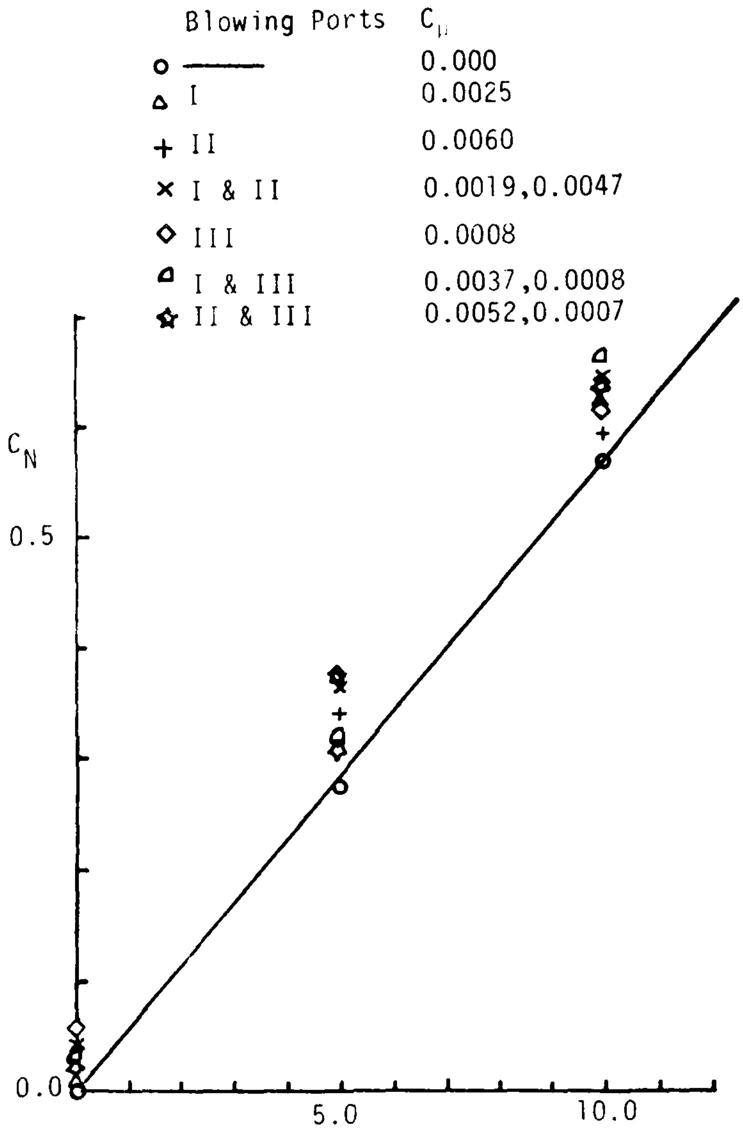

Figure 7. Normal Force Cver the Wing Integrated from C_p Data, for Various Conditions of Blowing.

3. WATER TUNNEL EXPERIMENTS

From the wind tunnel experiments, it appeared that the overall circulation of the wing was significantly altered due to a small amount of jet blowing. Moreover, the location of jet appeared to be sensitive in regards to the wing performance. The variation in flow field due to jet blowing must be observed and understood. For this purpose, qualitative observations of the flow field and the wingtip vortex rollup with and without tip jets blowing were investigated in the water tunnel. The flow visualization study was to aid in the understanding of the flow field perturbations due to the wingtip jet blowing.

Description of Facility and Model

The UTSI water tunnel is a closed circuit, continuous flow facility especially designed for high quality flow visualization. The circuit of the tunnel lies in a horizontal plane. The tunnel is powered by a one horsepower electric motor connected via a variable speed transmission to a 25 cm diameter, twin-bladed propeller in the return leg of the tunnel circuit. The transmission permits continuous variation in propeller rotational speed and continuous velocity variation from 2.5 cm/sec to 50 cm/sec (1 in/sec to 20 in/sec). The turbulence level in the test section is lower than 0.1%. The test section is 30.5 cm high, 45.7 cm wide, and 150 cm long (12 in. × 18 in. × 60 in.). All walls of the test section are made of plexiglass for versatility in observing and photographing the flow field.

The dye used was a mixture of alcohol, milk and commercial food coloring. Care is taken to insure that a specific gravity of unity is

achieved. The dye injection system consists of a pressure driven dye manifold that supplies dye to the model through 1.7mm (.067 in) diameter vinyl tubes. dye could also be injected upstream or downstream of the model through several moveable dye probes.

This wing model was also NACA 0012-64 airfoil section with semi-span of 27.4 cm (10.75 in.) and chord of 16.2 cm (6.375 in.). This was about nine-tenth scale of the wind tunnel model. One end of the wing was mounted to a shaft which extended through the side wall of the water tunnel. Model angle of attack was controlled by this shaft and measured by a geared counter assembly exterior to the tunnel. Wingtip jet ports were located at the other end of the wing which was at 60% of the width of the tunnel.

The geometry of the wingtip jet model used in the water tunnel was similar to the wind tunnel model. Table I describes the details of the wingtips used in the water tunnel investigation. These wingtip models were designed to test different wingtip jets effects on vortex rollup and to assess the influence of jet induced interaction in the near flow field about the wingtip. The jet ports were not contoured surfaces but simple openings machined through the tip into the water reservoir on the interior of the wing.

A concern in this test was the interaction of the jet with the water tunnel walls. To assess this problem, the method of Fern and Weston (Reference 24) was used to compute the undisturbed path of the jet centerline. For higher values of jet coefficient ($C_\mu > 0.05$) the undisturbed jet was predicted to strike the tunnel side wall within the test section region. This was investigated experimentally by placing the

TABLE I

WATER TUNNEL JET CONFIGURATIONS

Configuration Designation	Configuration Design Parameter	Photographic Series	Sweep Angles* δJ_1	Sweep Angles* δJ_1	Sweep Angles* δJ_1	Dihedral Angles** λ_1	Dihedral Angles** λ_2	Dihedral Angles** λ_3	Jet Shape
I	Baseline	J and D	135°	90°	45°	0	0	0	
II	Sweep Angle	B	150°	90°	60°	0	0	0	
III	Dihedral	C and F	135°	90°	45°	-30°	0	30°	
IV	Jet Shape	E	135°	90°	45°	0	0	0	

*Sweep angle measured along free stream direction in X-coordinate

**Dihedral angle positive for upward blowing.

wing at zero angle of attack and the dye in the jet itself to see if the undisturbed jet approached the side wall. At $C_\mu = 0.05$ the jet was approximately 2 inches from the wall as it left the test section. It is expected that this deviation from a prediction based on well established data is attributable to wall interference. Indeed, for the extremely large jet coefficients, outside the data range of the experiment ($C_\mu > 0.5$), wall interference was obviously present since the actual impingement of the jet on the wall could be seen.

However, it is very important to note that these observations as well as the theoretical prediction mentioned above are for an undisturbed jet. In particular, the influence of a strong vortex near the origin of the jet and running parallel to its path was not included. Observations in the water tunnel clearly showed that when the wing assumed a nonzero angle of attack and began producing lift, the jet trajectory was invariably pulled back toward the wing and away from the wall. Obviously the effect of the wing tip vortex was to greatly reduce the potential for wall interference. Thus two criteria proved to be important in minimizing wall interference: realistic jet coefficients ($C_\mu < 0.3$) and the production of lift (especially for $C_\mu > 0.05$). Within these limitations the influence of the wall is of negligible importance with respect to the interactions between wingtip jets and wingtip vortex in the present experiments.

Flow visualization was achieved by dye injection through several small ports located at the tip of the wing and on the lower surface of the wing. Water to the three jet ports was supplied from a water line via three tubes. The flow rate in each tube was measured by a

flowmeter. Many various combinations of jets were investigated.

4. WINGTIP JET INDUCED FLOW FIELD OBSERVATIONS

The wingtip wake flow was made visible, using dye injections from small holes on the bottom surface of the model, at incidence angles of 0^o to 12^o in the water tunnel. The dye was introduced on the model surface in the neighborhood of the wingtip and therefore the tightly twisted tip vortex core region was made visible. The wingtip vortex was extended far downstream with little or no diffusion. This vortex core flow is shown in Figure 8. With the wingtip jets blowing, the tip vortex core was dispersed significantly Figure 9. Depending on the jets blowing combinations and the amount of blowing, various degrees of dispersion was reached. Maximum dispersion was usually obtained with all three jets turned on (Figure 10).

The tip vortex core responded immediately to the jet blowing. Top view of a time sequence of the jets turned on and then off is shown in Figure 11. Note the dye trace from the moveable probe which was placed about one-half inch away from the corner of trailing edge of the wing was completely trapped and mixed with the diffused trailing vortex flow but separated immediately from it as soon as the jets were turned off. This indicated that the jet blowing had a tendency of diffusing the tip vortex flow.

This investigation was undertaken to learn more details on the physical process of the flow around the wingtip. Therefore, careful observation of every pattern was necessary; both to identify its source and its effects. In the water tunnel study, larger jet coefficients compared to the wind tunnel study were used for better visualization and

Figure 8. Persistent Wingtip Vortex Flow.

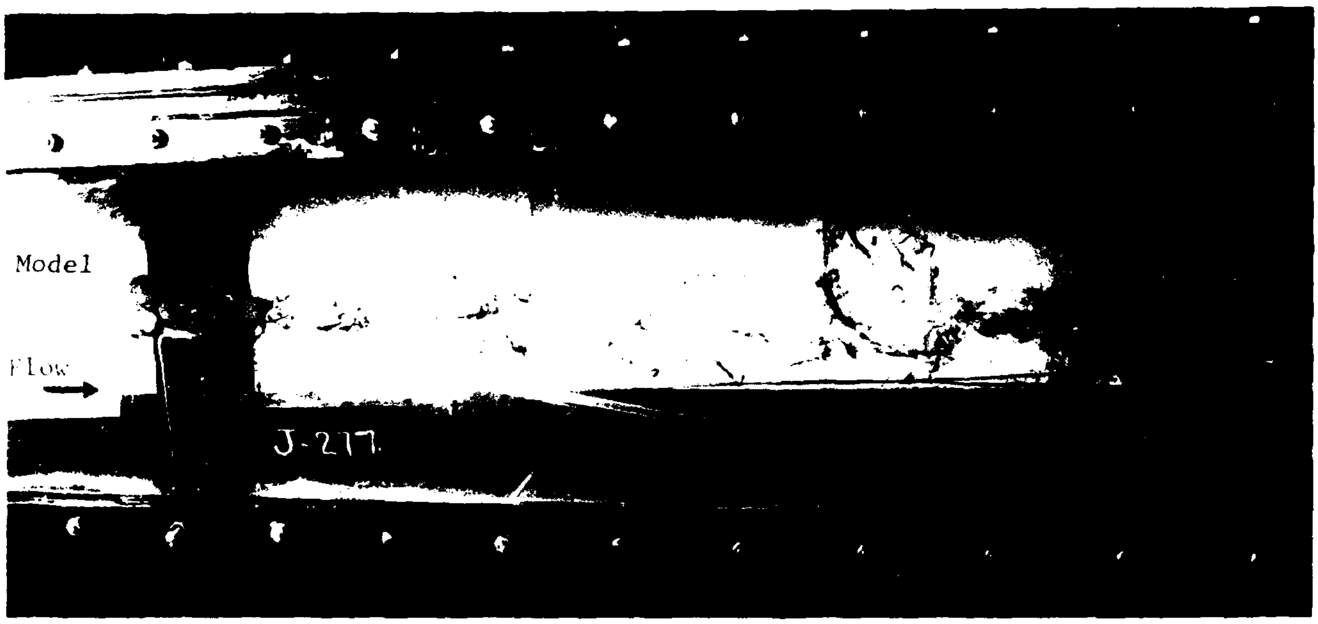

With Jet Blowing from Front Port
(Note the Secondary Vortices Rotating Perpendicular
To Free Stream)

Figure 9. Wake Flow Field with Jet Blowing.

Wi

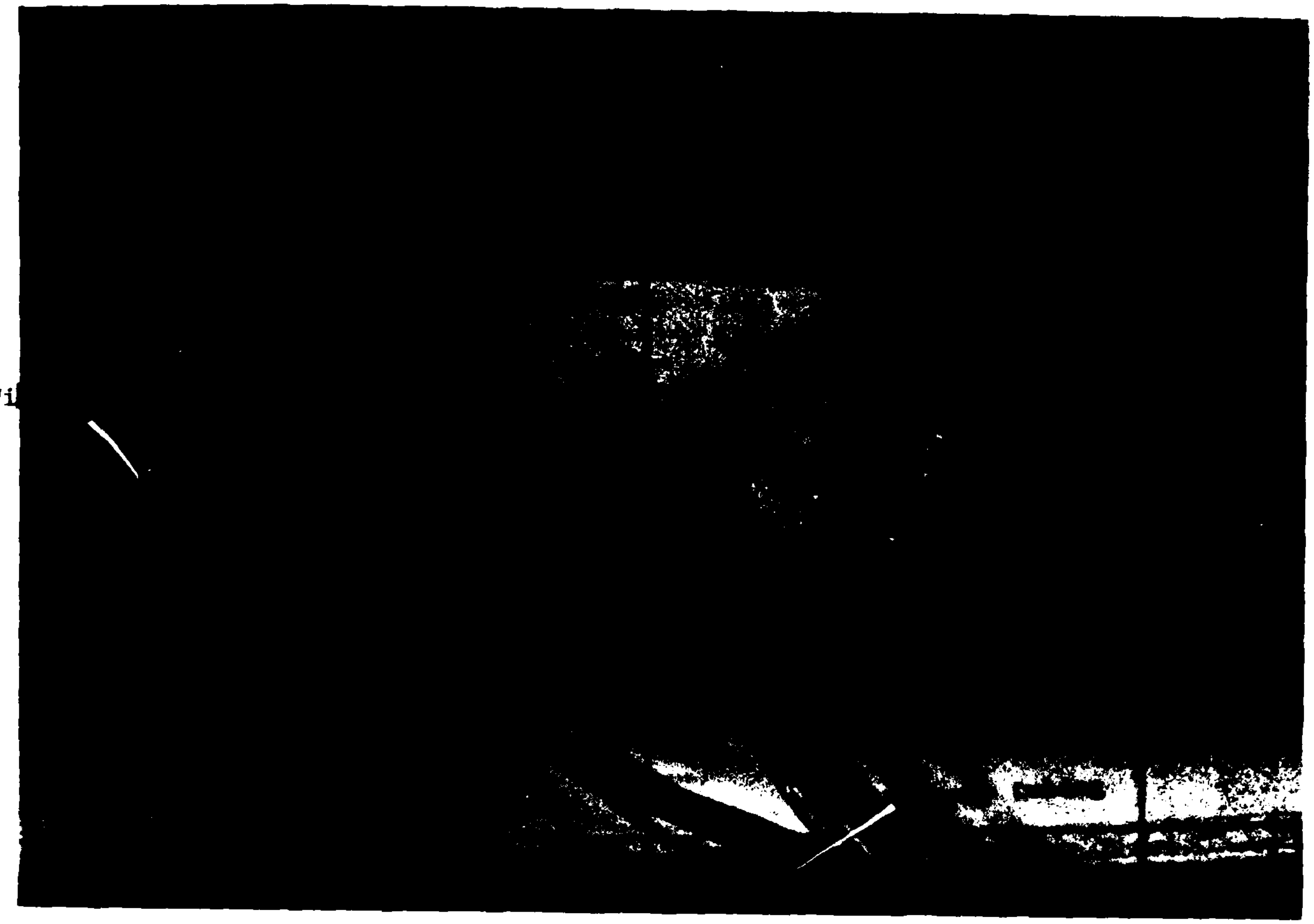

Figure 10. Maximum Dispersion of Vortex Wake Flow with All Three Jets Blowing.

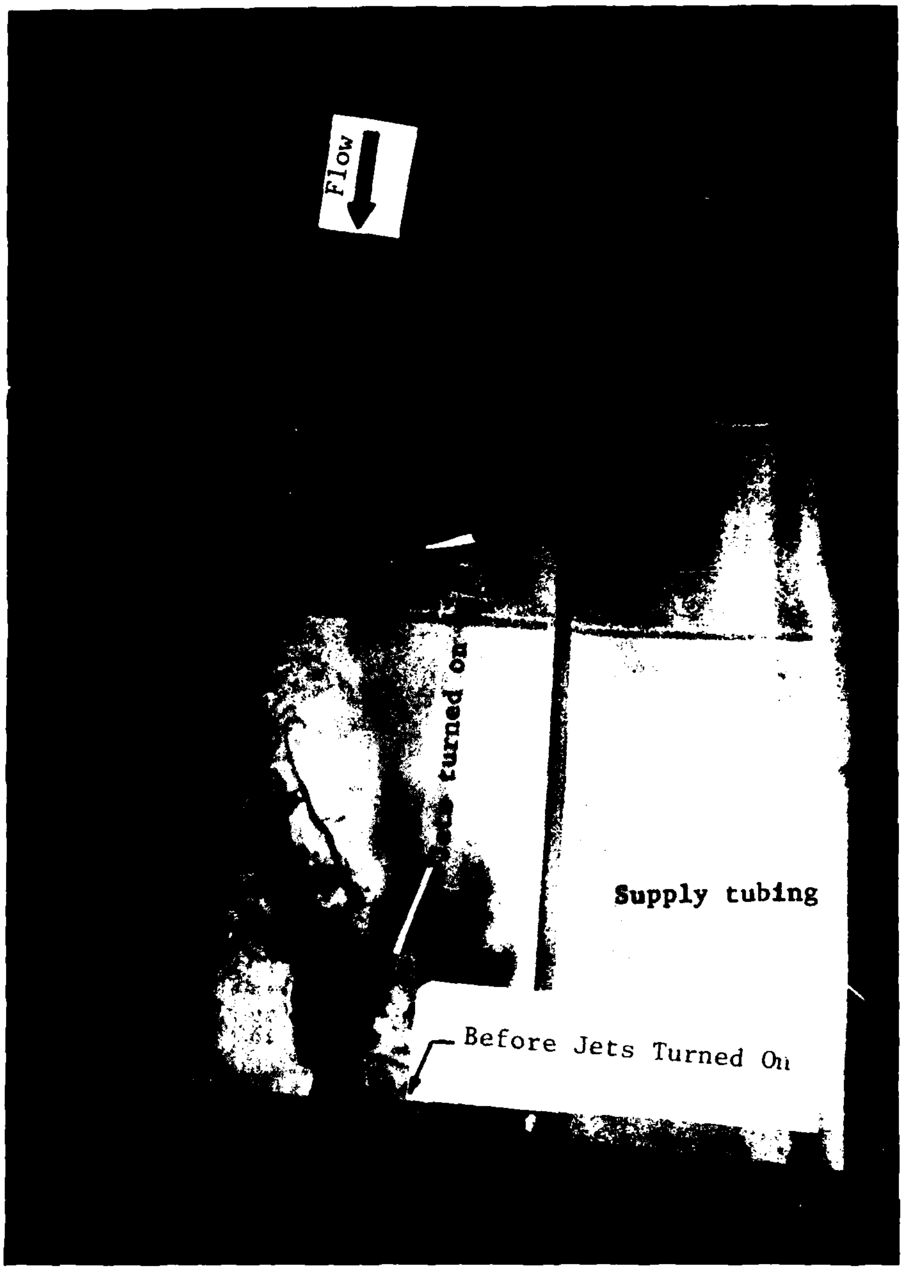

Top View

Outboard Shift of Vortex

Figure 11 . Time Sequence of the Jets Turned On, Then Off.

enhancement of the interactions observed. Many peculiar processes were present and each were investigated in detail. The important observations on the unexpected phenomenon with some understanding of their influence are elaborated on in the next sections.

Description of the Secondary Vortices

An unexpected result of the flow visualization tests was observation of the production of many different types of secondary vortices in the wake region. These vortices can be catagorized into three types and will be explained in detail below. When the jets were blown from all three ports, the induced turbulence was so strong that the observation of the above mentioned details became difficult. For better flow visualization, jets were blown in a carefully controlled manner from each jet port.

1. Observation of "Spin-off Vortices"

Interesting, periodically spaced and fast spinning secondary vortices were observed when mildly strong blowing from the front jet port (port# 1) was present. These secondary vortices had the appearance of a "cyclone" or a 'tornado' with their axes perpendicular to the tip vortex flow and to the main flow (Figure 12). We call this type of secondary vortices the "Spin-off Vortices". Two side views and a top view of these spin-off vortices are shown in Figures 12-14.

In Figure 13, while turbulence was strong that most dyes disappeared, three of these laminar vorticores are clearly shown while a fourth is breaking apart. These vortices were formed in the very complex region of the flow at the tip near the trailing edge. Typically they

Figure 12. Strong Periodic "Spin-Off" Wake Vortices Produced By Front Port Jet Blowing with $C_\mu = 0.16$.

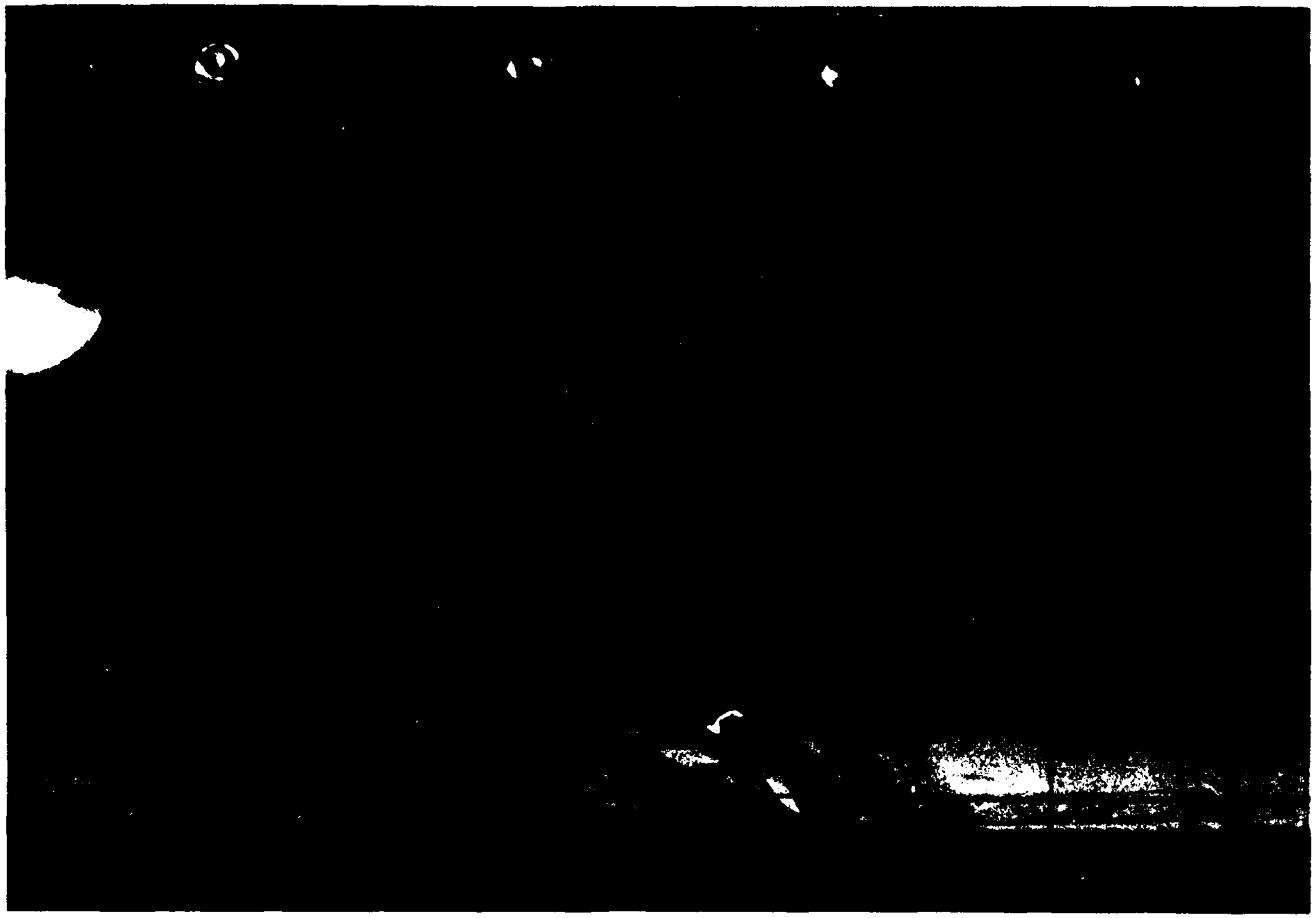

Figure 13. Periodic Auxiliary Vortices in the Wake Region. The Laminar Spin-Off Vortex Cores Visible Imbeded Within Turbulent Wake Flow.

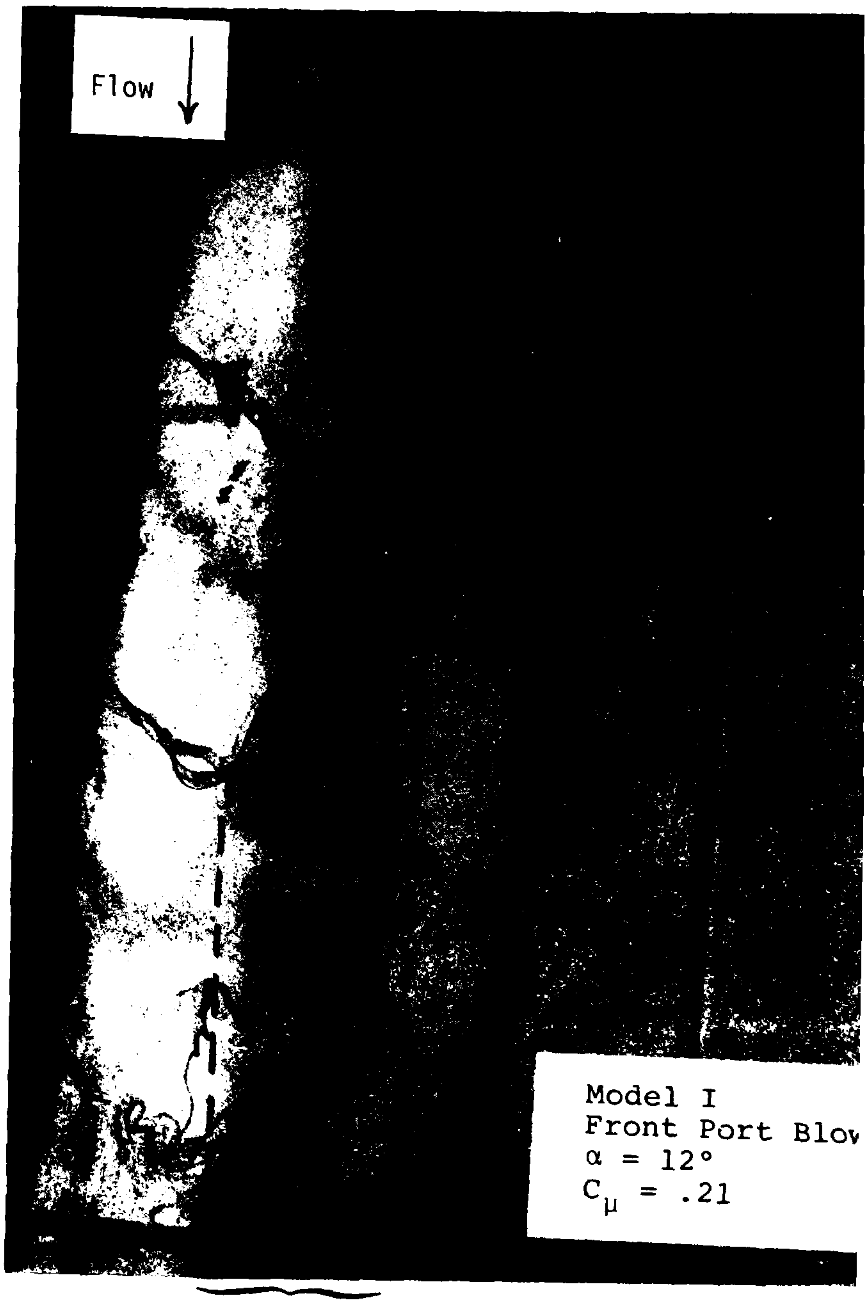

Apparent AR Increase

Figure 14. Top View of Periodic Auxiliary Vortices with $C\mu = 0.21$. Note the Increase In "Apparent As In Wake Flow.

would emerge from the rolling up tip vortex as a loosely wrapped, swirling dye streak rotating counterclockwise about the Y axis. Each secondary vortex would then be stretched in the positive Y direction and would gradually assume a tighter spiraling path as its rotational speed increased. At a point outboard of the wing the secondary vortices were deflected so that their path and rotational vector were aligned with the Z axis. At about this same time the speed at which the tip of the secondary vortex was moving would increase dramatically to a speed that appeared to exceed free stream velocity. The dye marking the tip of the vortex steadily developed a more pointed shape as the vortex was stretched, and the rotational speed of this tip region continued to increase until the streakline abruptly stopped at a position as shown in Figure 13. These vortices appeared to emerge from the rolling up wing tip vortex, and because of their rapid spinning, they were called "spin-off vortices".

A top view of the spin-off vortices is shown in Figure 14. This photograph of the baseline model with front port blowing at $C_\mu = 0.21$ shows one vortex just forming slightly ahead of the trailing edge and three fully developed and regularly spaced vortices.

Periodic spin-off vortices occurred only when moderate blowing from the front jet port was used. Jet coefficients of approximately 0.16 were most effective at producing distinct periodic secondary vortex patterns. Secondary vortices were not associated with blowing from the middle or aft jet ports.

A singular secondary vortex identical to the periodic ones was often found to occur when front jet port was initiated. This vortex

appeared at much lower jet coefficients but only as the initial jet surge was emitted. No indication was ever seen that successive secondary vortices were trying to develop in a periodic pattern. Cycling of the jet valve was found to produce a succession of these singular vortices in a controlled periodic pattern.

The periodic secondary vortices were much more prominent for the baseline model and model III than for other configurations. In particular, model II, with the modified jet sweep angles, produced secondary vortices that were poorly defined if even discernible. This was true despite extensive searching for a combination of blowing coefficient, dye port locations and angle of attack that would make the secondary vortices visible.

The spin-off periodic vortices are attributed to the unsteadiness caused by the wake generated behind the front port jet. The oscillation of jet wake had periodic 'entrainment' or 'sweeping' effect on the vorticity generated on the wing surface. This results in spin-off vortices perpendicular to the main flow. These vortices moved far away from the main tip vortex core region into the free stream region and are therefore a means of weakening the wake vortex.

Time sequence photos (Figure 15 a,b), where two pictures were taken two seconds apart, indicate the development of a smaller spin-off vortex in between the two larger spin-off vortices. The vorticity contained in a smoke-ring-like local flow finally evolved into a fast spinning cyclone type vortex flow. Note that a new vortex ring appeared in approximately the same period at the left side of Figure 15 b. Undoubtly, these periodic spin-off vortices have a significant impact on the disper-

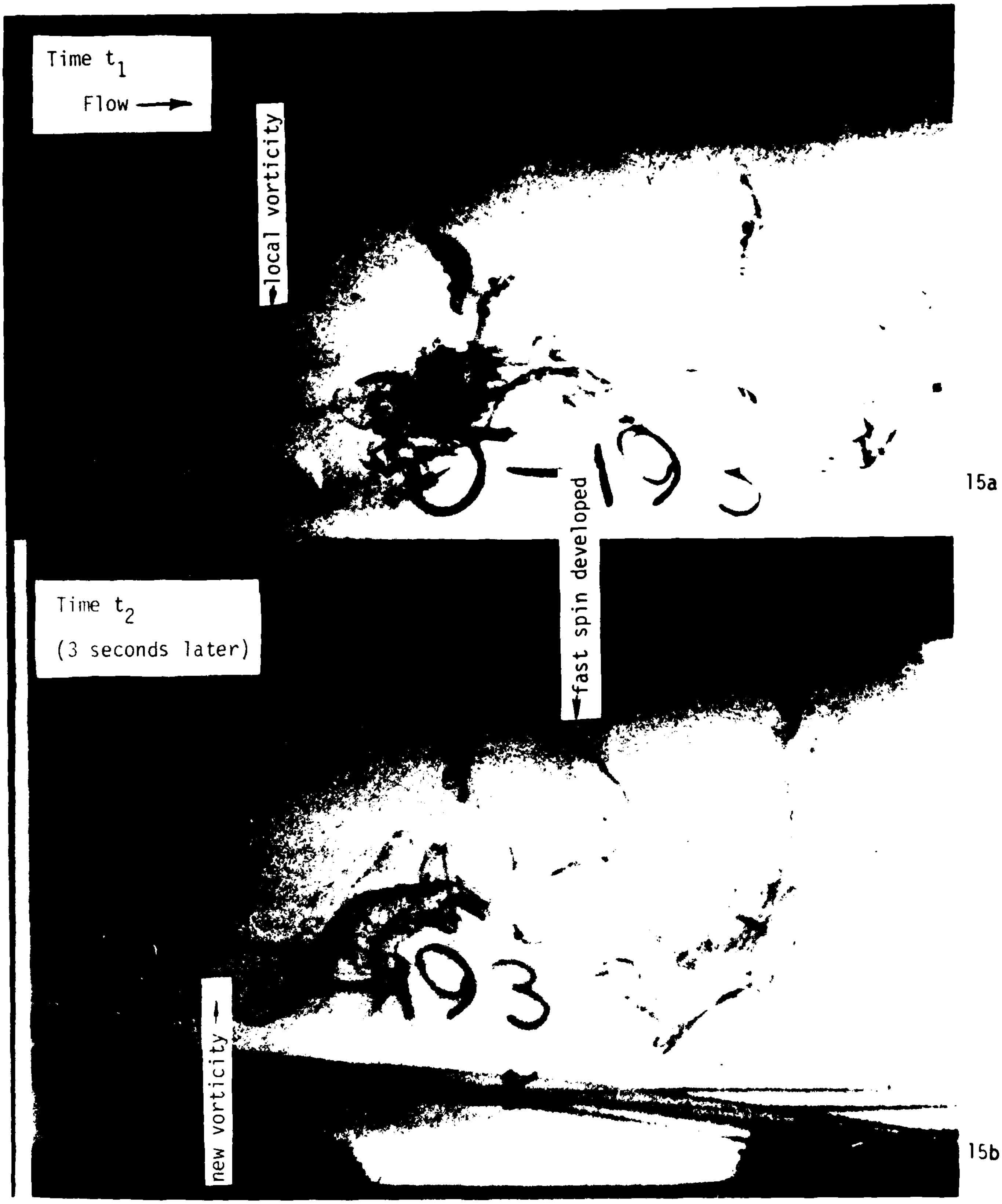

Figure 15. Time Sequence of Development of Secondary "Spin-Off" Vortices.

sion of the tip vortex.

If one carefully observes the Figure 14, it reveals also that the wake flow has moved outboard significantly. This is corresponding to the increase of apparent aspect ratio of the wing. Again, such a wake flow would alter the overall circulation on the wing as a consequence.

2. Observation of Counter Rotating Vortex Pair

Two counter rotating vortices characteristic of a jet in a cross flow were frequently seen during the water tunnel testing. Figure 16 shows a typical pair, this photo is taken for the single jet from the aft port at $\alpha = 0^o$. These jet vortices appeared immediately after the jet left the orifice. When the jet was placed at positive angle of attack, one of the jet vortices appeared to be stronger than the other. This is attributed to nonuniform flow around the tip and therefore around each geometrically skewed jet. Frequently, one of these vortices was drafted into the wingtip vortex, near the jet exit, and disappeared. The stronger vortex (the other half of a pair, due to a skewed jet in the cross flow) was lifted and gradually wrapped around the wingtip vortex. A close-up view of flow field near jet port 2 and 3 is shown in Figure 17. In this figure, the jets were blown only from the ports 2 and 3. The dye from the bottom surface of the wing has been captured into the jet blown from the port 3 but missed the jet from the port 2 in this typical photo. This phenomenon became visible only when the dye was in the right location with respect to the jet.

Figure 18 is a photo indicating this counter rotating vortex (opposite to the tip vortex rotational sense) interacting with the tip vor-

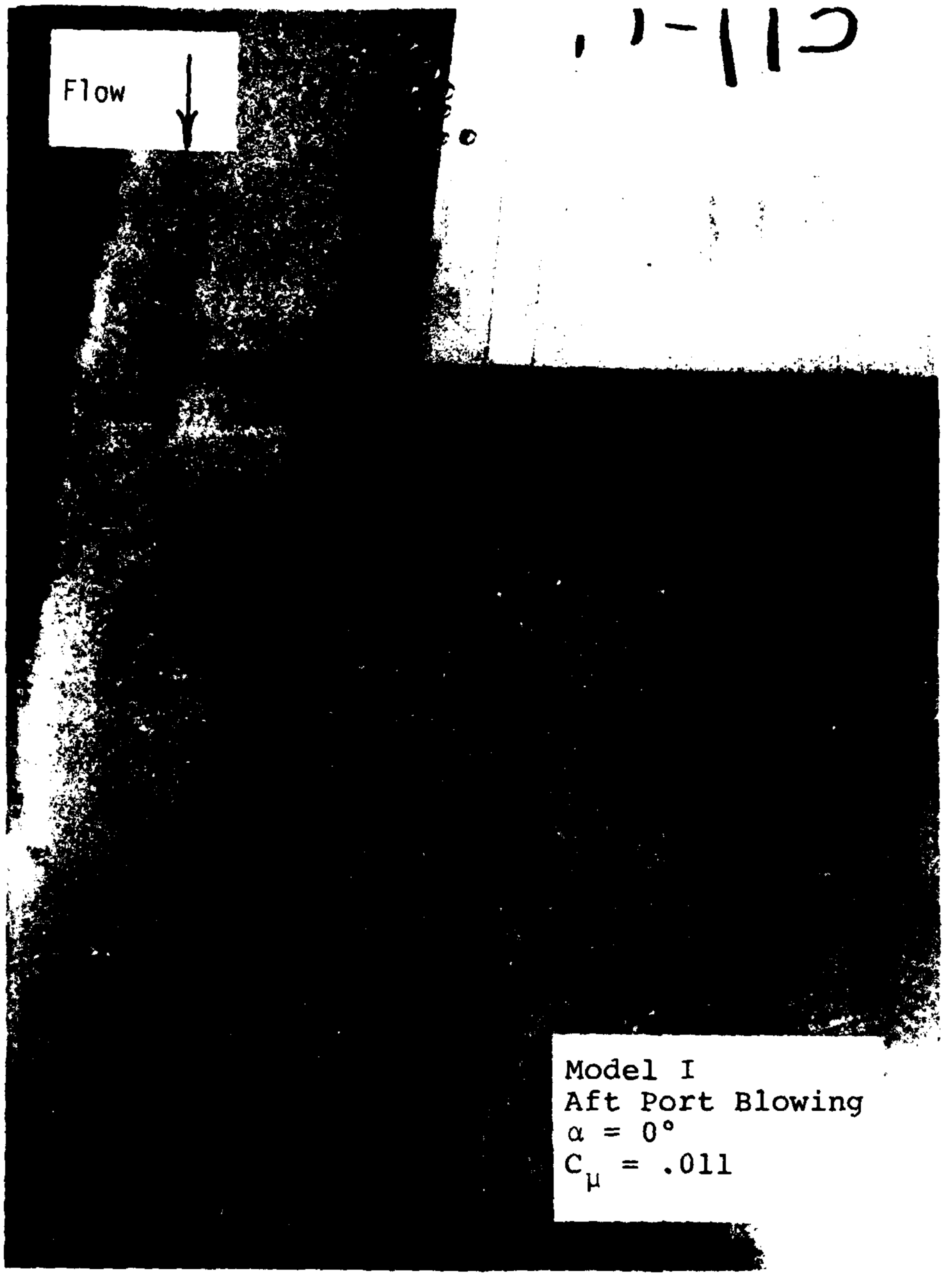

Figure 16. Top View of Counterrotating Vortex Pair By Jet (with a Symmetric Wing at $\alpha = 0^o$)

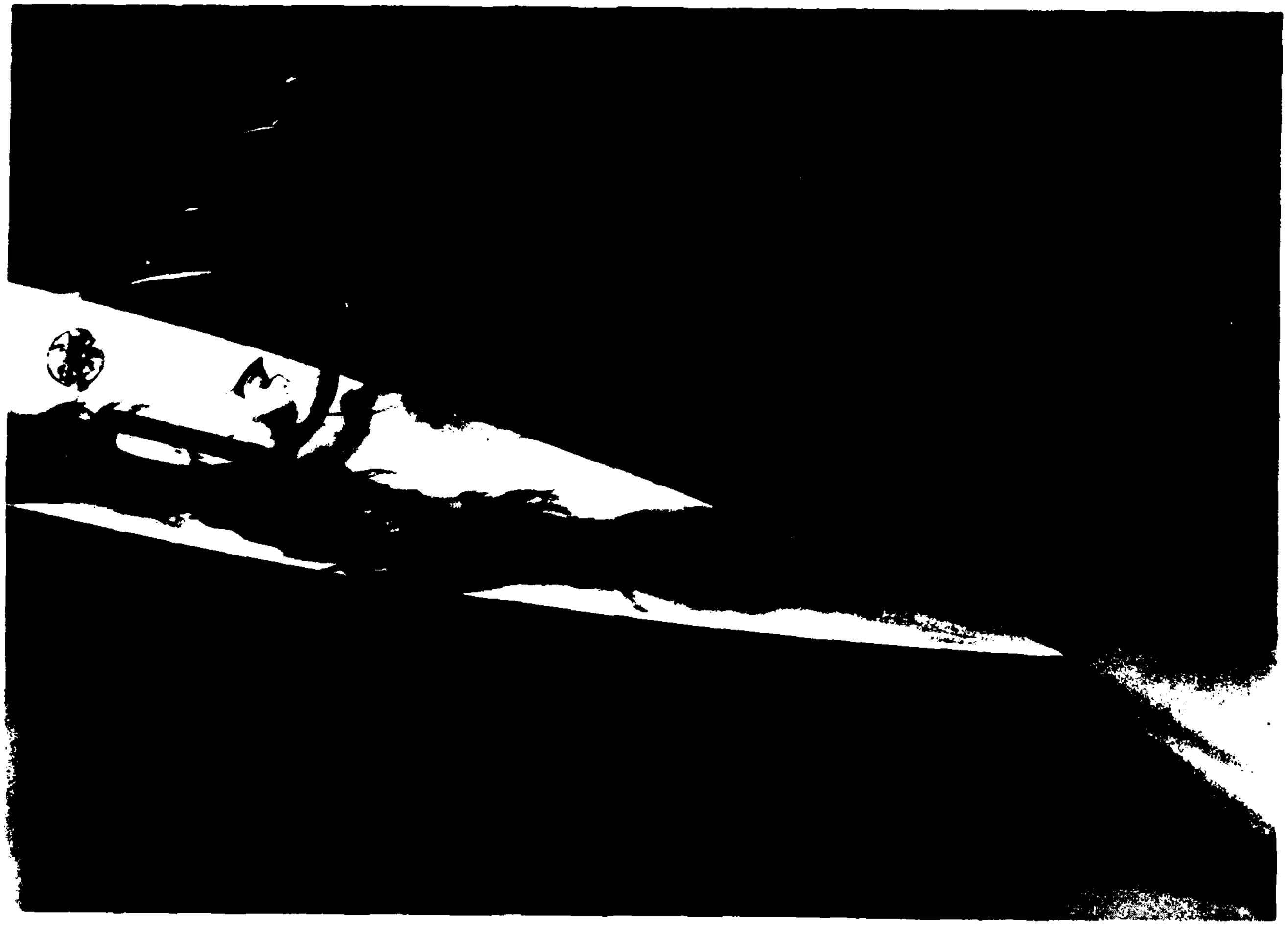

Figure 17. Counterrotating Auxiliary Vortex Flow (Close Up View of Jet Ports #2 and #3).

Figure 18. Downstream Interaction of Counterrotating Auxiliary Vortex and Wing Tip Vortex Flow.

tex flow at downstream. A violent nonlinear interaction was usually observed

whenever these two counter rotating vortices merged together. The intermediate interactions, before the final merge, are shown in Figures 19-21. The gap between two vortices are increased slightly from Figures 19 to 21. The streak lines of the two vortices themselves as well as the region of mutual interactions between the two vortices are visible.

From these observations, it was clear that the interaction between vortices were nonlinear. The onset of tip vortex flow has been significantly altered by the presence of this counter rotating "auxiliary vortex" due to the asymmetricity of a pair of vortices generated by the jet! This gave us a hint to establish a theoretical model in computing the roll-up of tip vortex flow with presence of a pair of counter rotating vortex singularities. The development of theory as well as its result will be presented in the analysis section later.

As mentioned earlier, if the dye location was proper such that the dye could be trapped into the jet blown from the port 2 and 3, two distinguished auxiliary vortices were visible. Both vortices were rotating in the opposite sense to the tip vortex flow. This is shown in the Figures 22-23. In general, this type of counter-rotating and nearly parallel to the free stream "auxiliary vortex" was observed when the jet was blown from the aft ports (i.e., port 2 or 3). When jets were blown from all three ports the turbulent mixing became so strong that the flow field appeared very smoky, and only random and broken laminar streak line segments were observable (Figure 24).

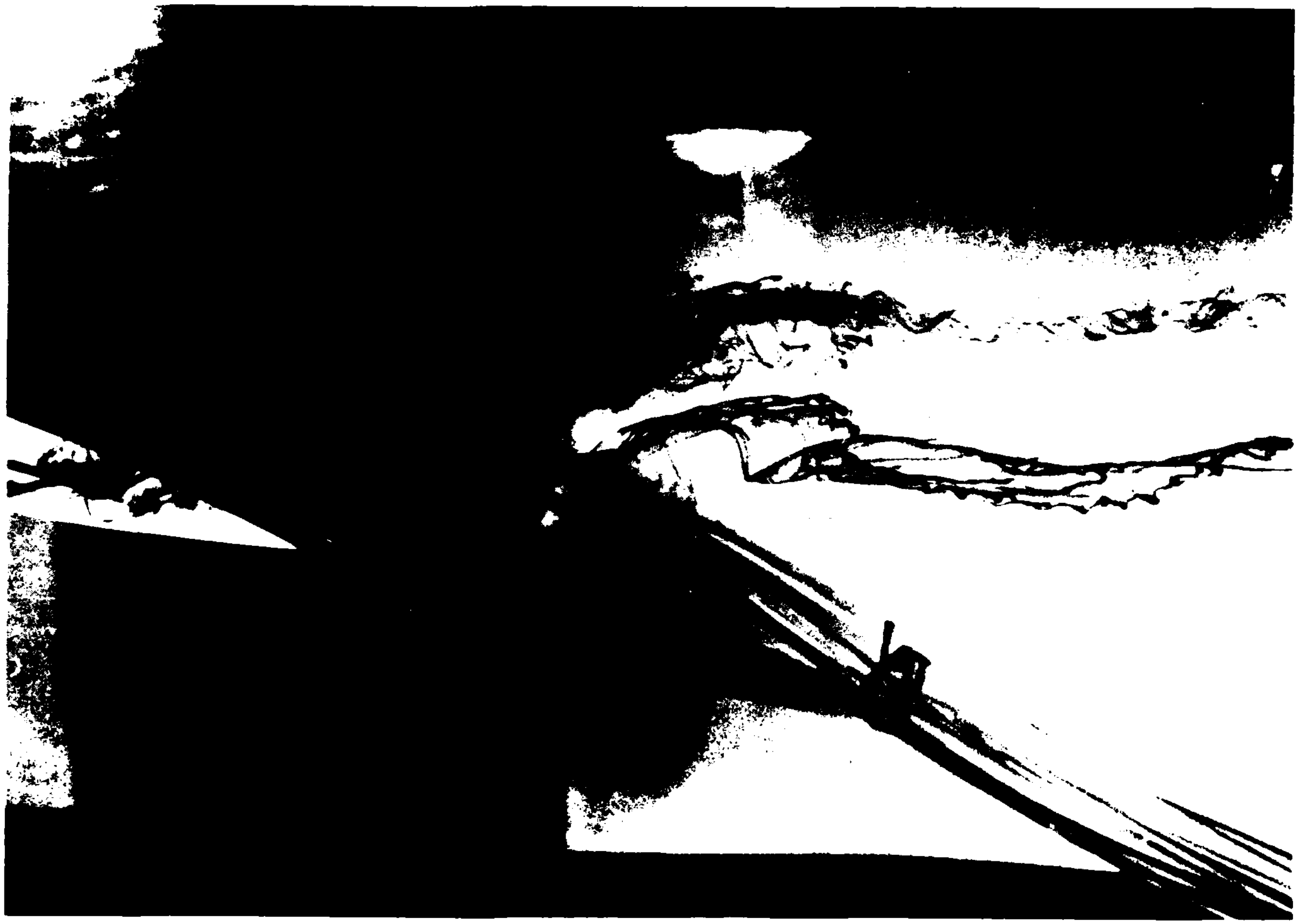

Figure 19. Interaction of Counterrotating Auxiliary Vortex and Tip Vortex Flow.

Figure 20. Detail Flow Structure of Counterrotating Auxiliary Vortex and Its Interaction.

Figure 21. Streak Lines Show the Interaction of Two Vortices Coupling.

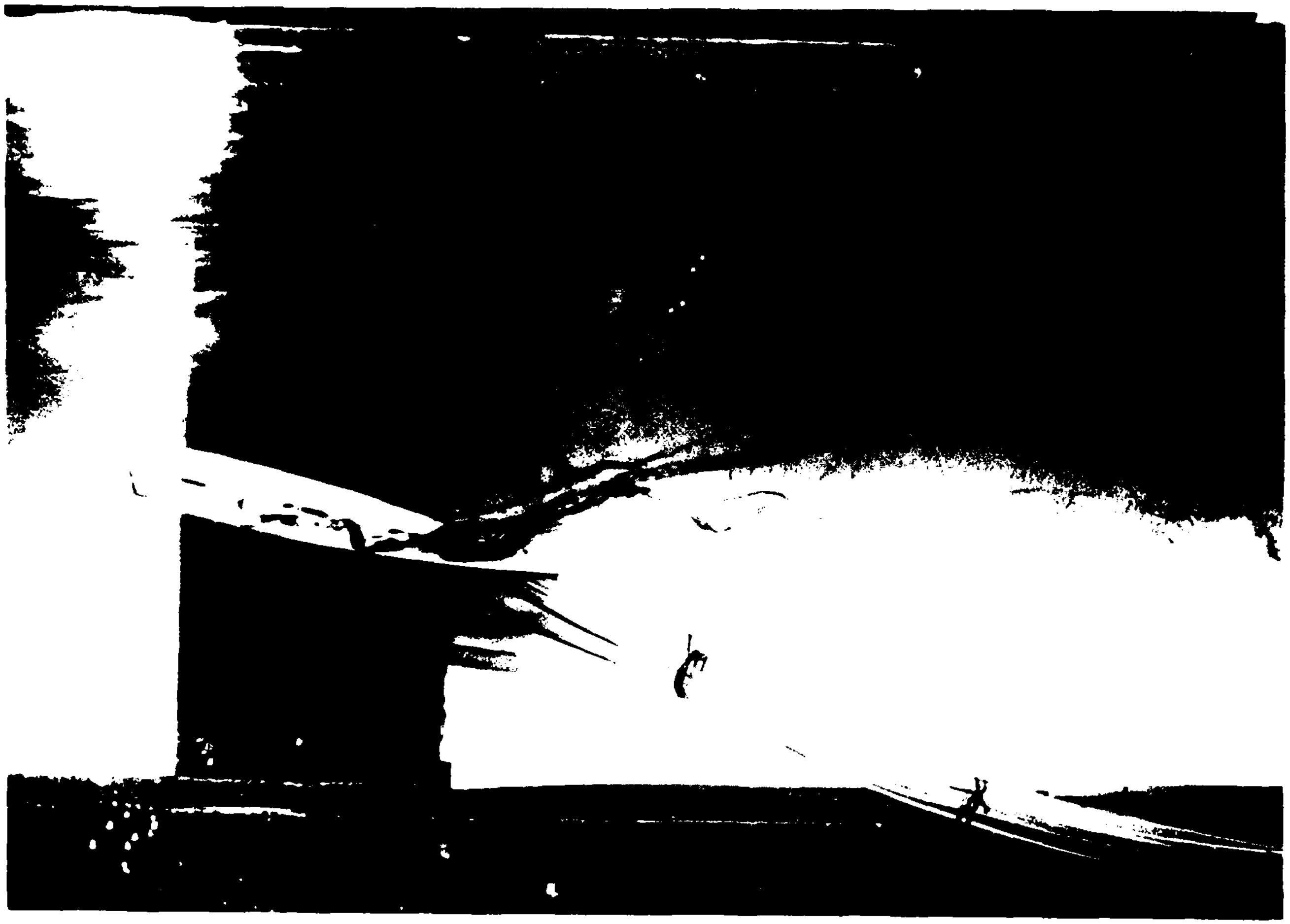

Figure 22. Multiple Counterrotating Auxiliary Vortices Interacting with Wing Tip Vortex Wake Flow.

Figure 23. Counterrotating Auxiliary Auxiliary Vortices Due to the Multi-port Jet Blowing.

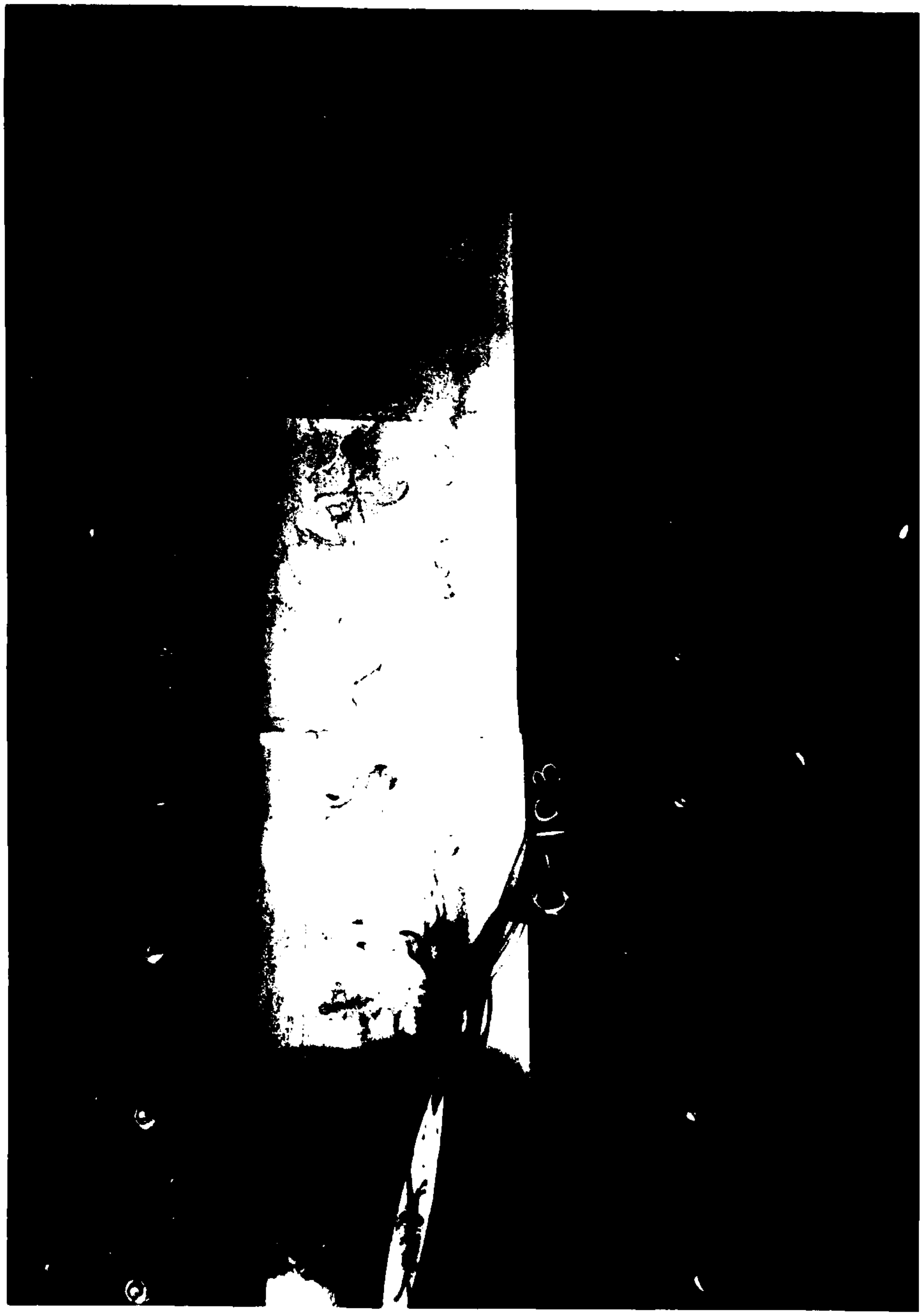

3. Entrained Secondary Vortices

A different type of periodic vortices was observed while testing model IV, with the aft port blowing the vertical jet slit model. These were characterized by vortices bound at one end to the wing tip vortex and the other end to the jet vortex (Figure 25). These secondary vortices would stretch as the jet vortex and tip vortex traveled apart due to the relatively heavy blowing. Since photographs of this event did not show the details, Figure 26 shows the observed structure illustrated.

There was an increase in mixing due to the presence of these vortices. The dye was entrained from the wingtip vortex into the entrained vortices, and thus we called these "Entrained Secondary Vortices." These observations were not made with any other model.

Other Observations and Comments

All of the secondary vortices draw a portion of their energy from the wingtip vortex and consequently reduce its strength. This process also creates more mixing in the wake region and thus hasten the decay of the entire vorticity. This is a major technique in generating dispersion of the wingtip vorticity in the wake.

Jet blowing produced two significant and distinct effects on the location where the wingtip vortex originated and its subsequent trajectory. Wind tunnel measurements showed that discrete wingtip jets under certain conditions increased the lift. This improvement is expected to provide reduction in induced drag. Therefore, the jet effects could be compared to a physical extension of the wing or an effective increase in the wing aspect ratio. We call this an "apparent aspect" ratio increase (See for example Figure 14). It will be shown later in the

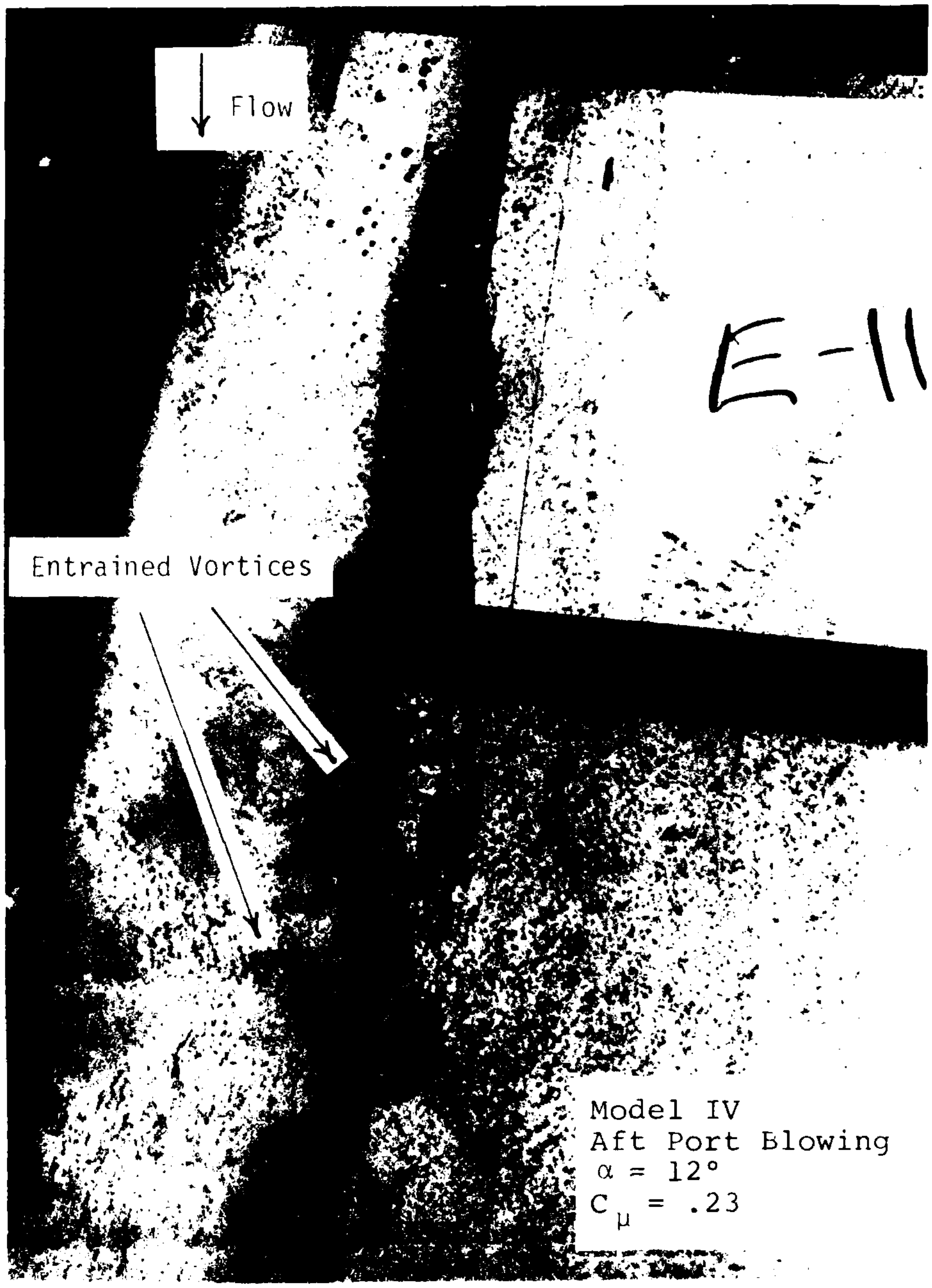

Figure 25. Entrained Vortices Between Jet and Tip Vortices.

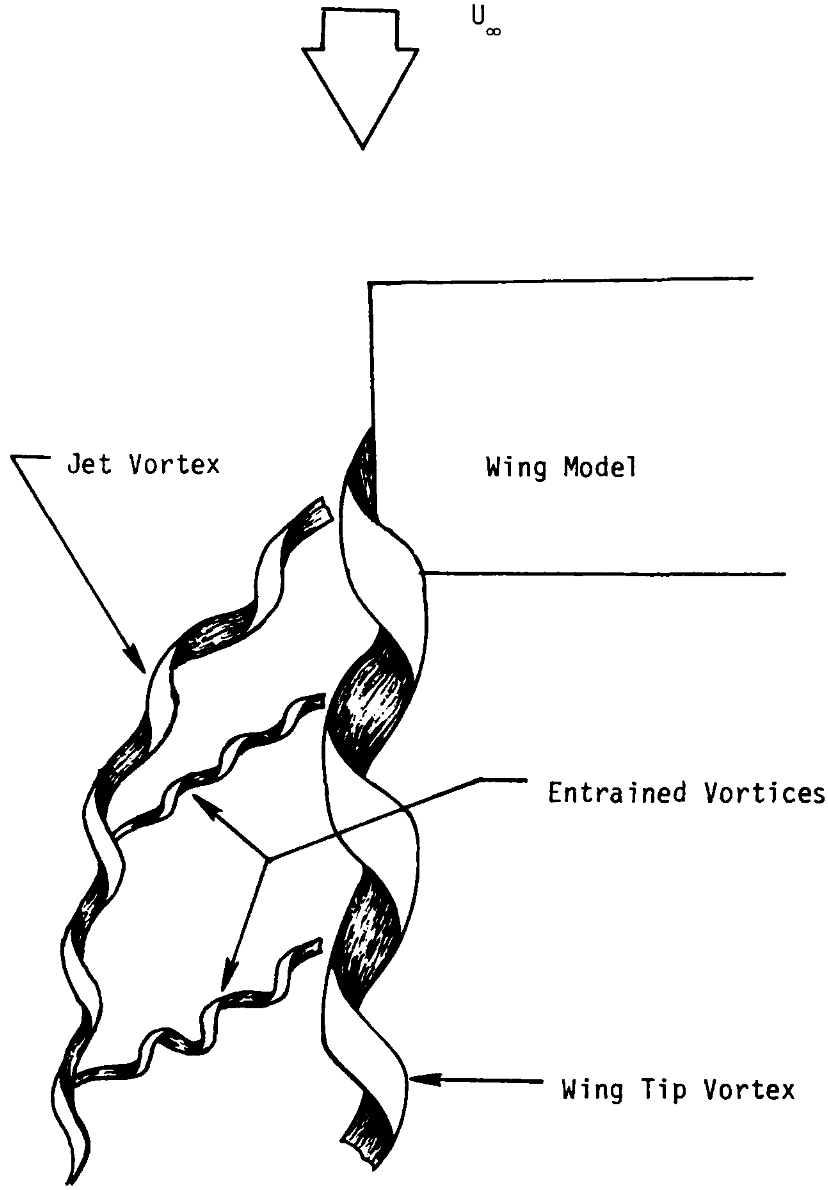

Figure 26. Structure of the Entrained Vortices.

tip vortex roll-up analysis section that the vortex singularities placed at the wingtip could effectively move the wake flow outboard. Thus, it is also equivalent in increasing the wing apparent aspect ratio.

It was observed that jet blowing did shift the wingtip vortex outboard even with very small amounts of jet blowing. Figure 27 a,b compares the vortex position as a function of jet coefficient for the baseline model at $\alpha = 12^o$ with the middle and aft port blowing. With $C_\mu = 0.0$ (no blowing), the wingtip vortex rolls up over the wingtip and moves inboard as shown. With small blowing, $C_\mu = 0.006$, the vortex was shifted outboard noticeably, and the vortex core was actually formed at a point beyond the wingtip. For larger amounts of jet blowing there were more dramatic changes present as evidenced in Figure 14.

A significant change in the vortex trajectory with respect to its path in the vertical plane was also observed. The main wingtip vortex was lifted up for almost all the blowing configurations (Figure 28). Unlike the outboard shift in the horizontal plane, this result was not expected. Initially this was thought to be possibly due to the dye buoyancy. On-line testing showed the dye to be neutrally buoyant, and tests at negative incidence angles confirmed that observation. The upward shift in the vortex trajectory was evidence of increase in the circulation that indicated a substantial improvement in the wing performance.

The aft jet port was somewhat more effective than the others in causing the wake vortex to be shifted upwards. Figure 29 shows model III with the rear jet blowing at a jet coefficient of 0.071. This is the wingtip that has the rear jet port at a positive dihedral angle, and the degree of upward motion may be influenced by the dihedral. However,

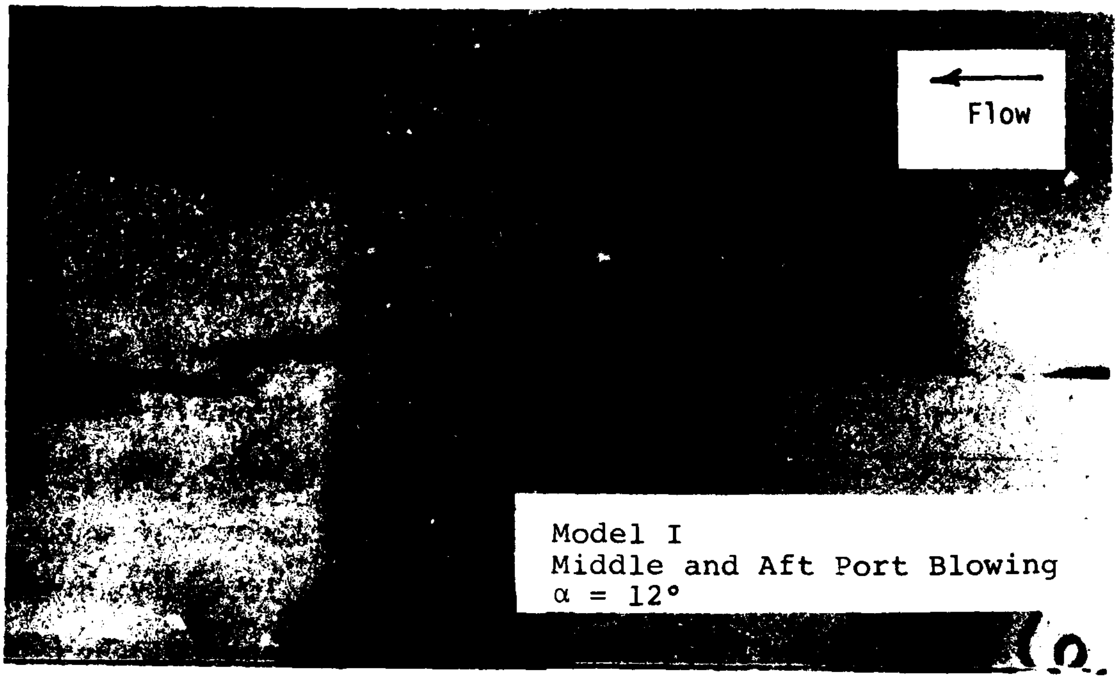

a. $C_\mu = 0.000$

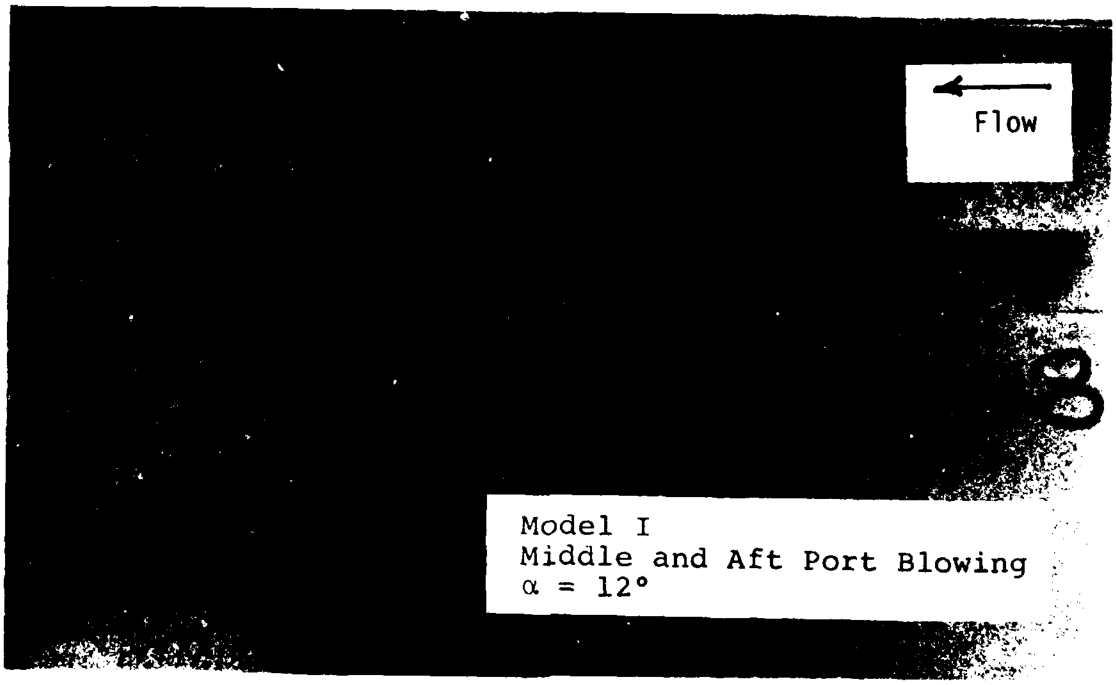

b. $C_\mu = 0.006$

Figure 27. Lateral Vortex Displacement

Figure 28. Upward Trend of Wake Due to Jet Blowing.

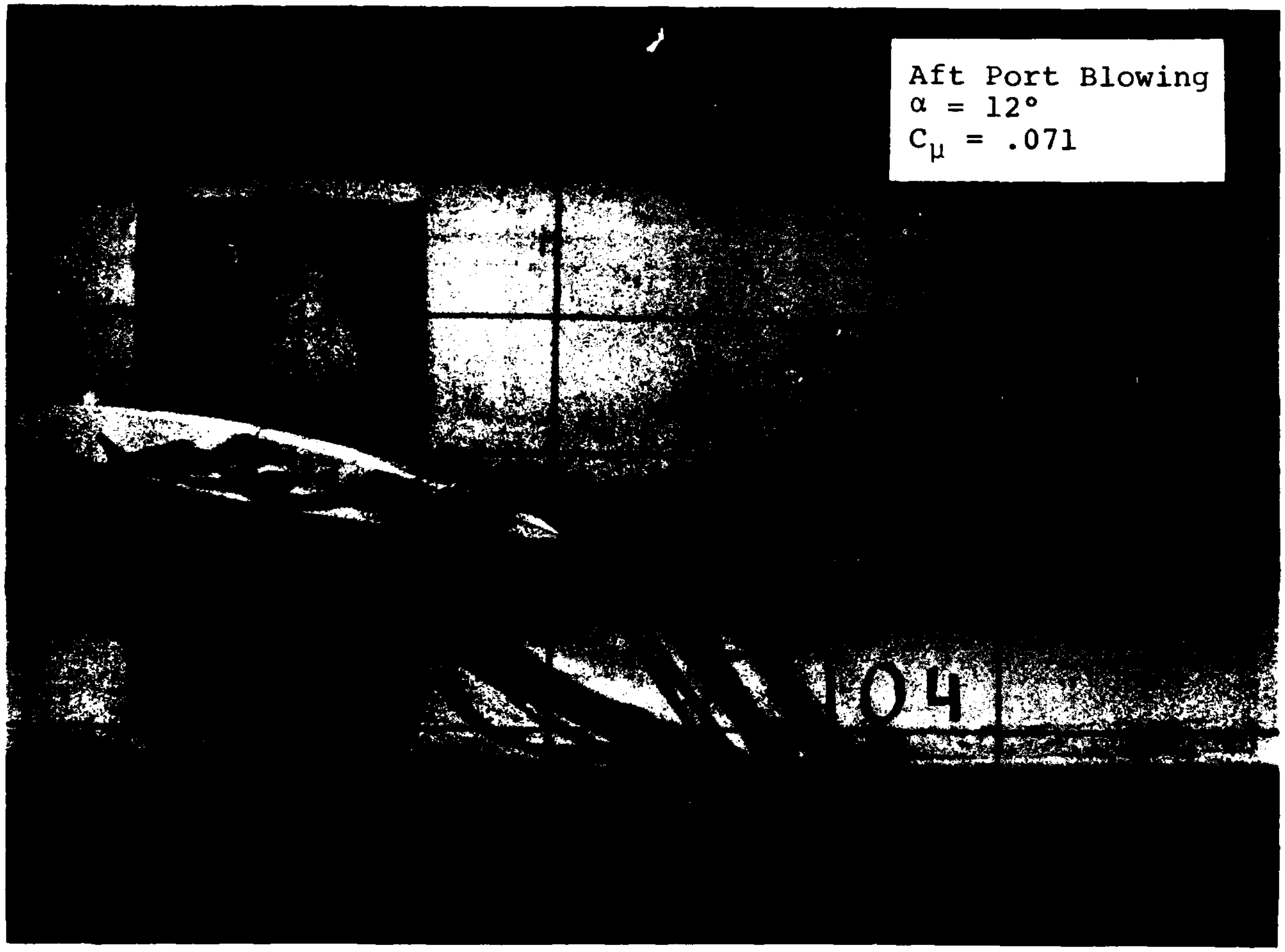

Figure 29. Vertical Vortex Displacement, Model III

other configurations with no dihedral showed vortex upward movement equally as large. Figure 30 illustrates this for the baseline configuration with rear jet blowing at $C_\mu = 0.050$. This baseline model showed that when aft port blowing was used the upward shift of the vortex increased steadily with jet coefficient C_μ. However, the greatest changes were seen at jet coefficients of 0.010 and lower. Increases beyond $C_\mu = 0.010$ caused very small changes in the trajectory.

Observations On Distributed Jets

A comparison of using equal amounts of mass flow of jets but distributed more toward the front ports and towards the aft ports is shown in Figure 31 a,b. It can be seen that quite different flow fields were observed. Distributed jet blowing also was effective in causing upward movement of the wake vortex. Figure 32 shows the vortex trajectory for model III with jet coefficients of 0.011, 0.011, and 0.003 respectively front to rear. The upwash was quite strong despite the fact that aft port blowing was light. However, distributed blowing patterns did not appear to be as effective as aft port blowing alone for equal combined jet coefficients.

The shift in vortex trajectory, and particularly the observation that the vortex remains elevated throughout the observable wake, indicates again that the jets may be altering the wing downwash. This apparent "upwash" seen in the wake should likewise influence the flow field ahead of the wing. It was difficult to measure the downwash distribution behind the wing in the present experiments. However, the analytical result indicates that the uplift of tip vortex would result in reduction of the downwash. This point will be elaborated on later.

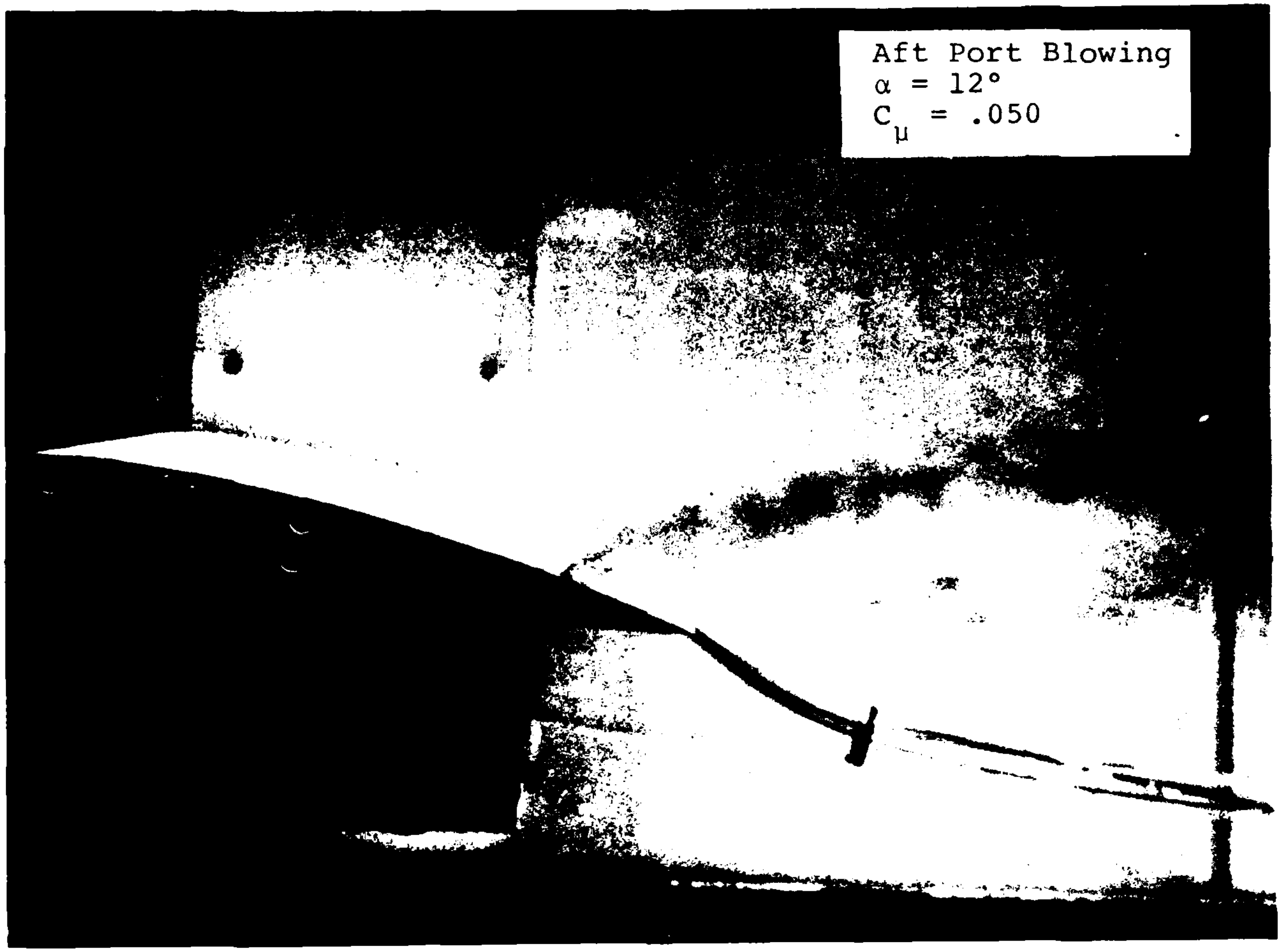

Figure 30. Vertical Vortex Displacement, Model I

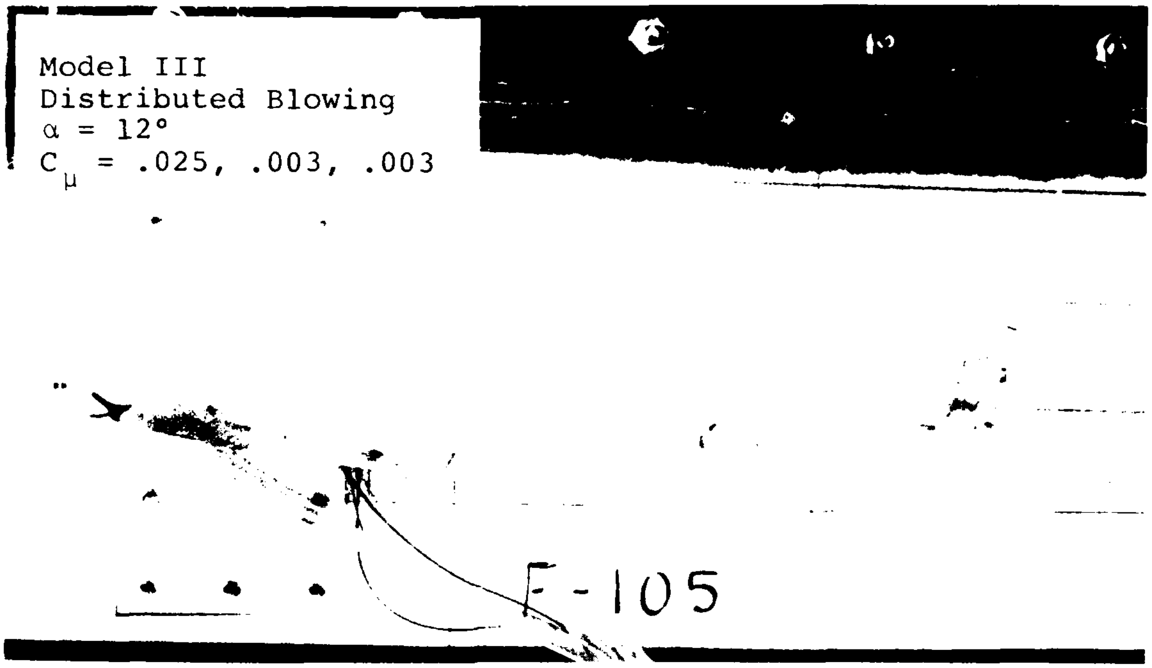

a. Blowing Concentrated Toward the Front

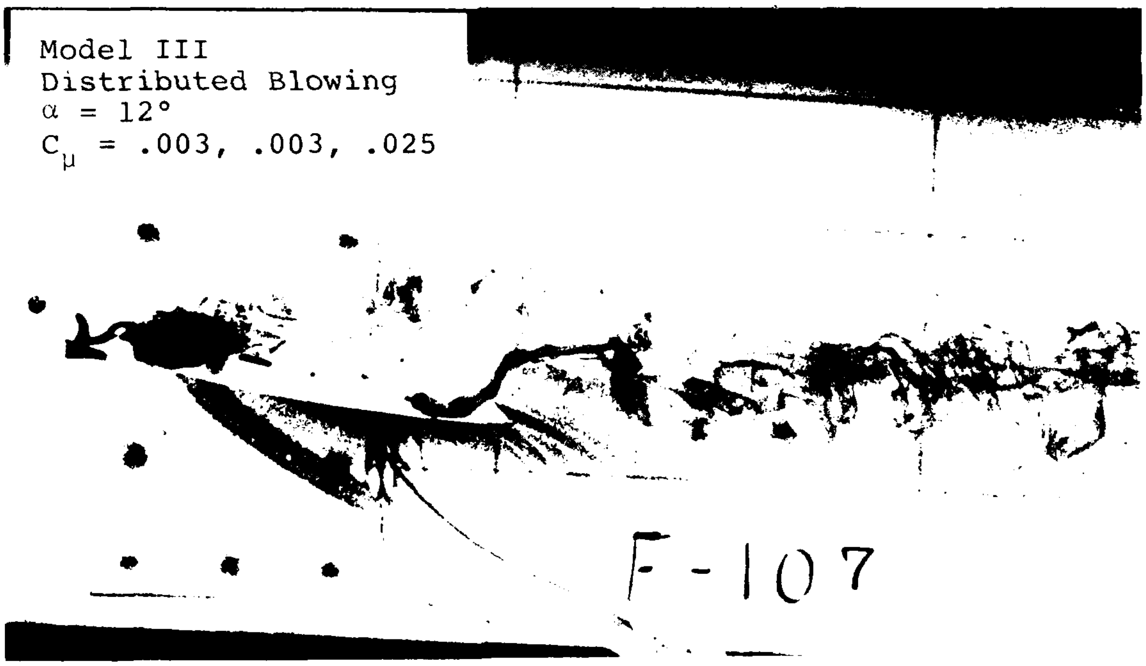

b. Blowing Concentrated Toward the Rear

Figure 31. Comparison of Blowing Distributions

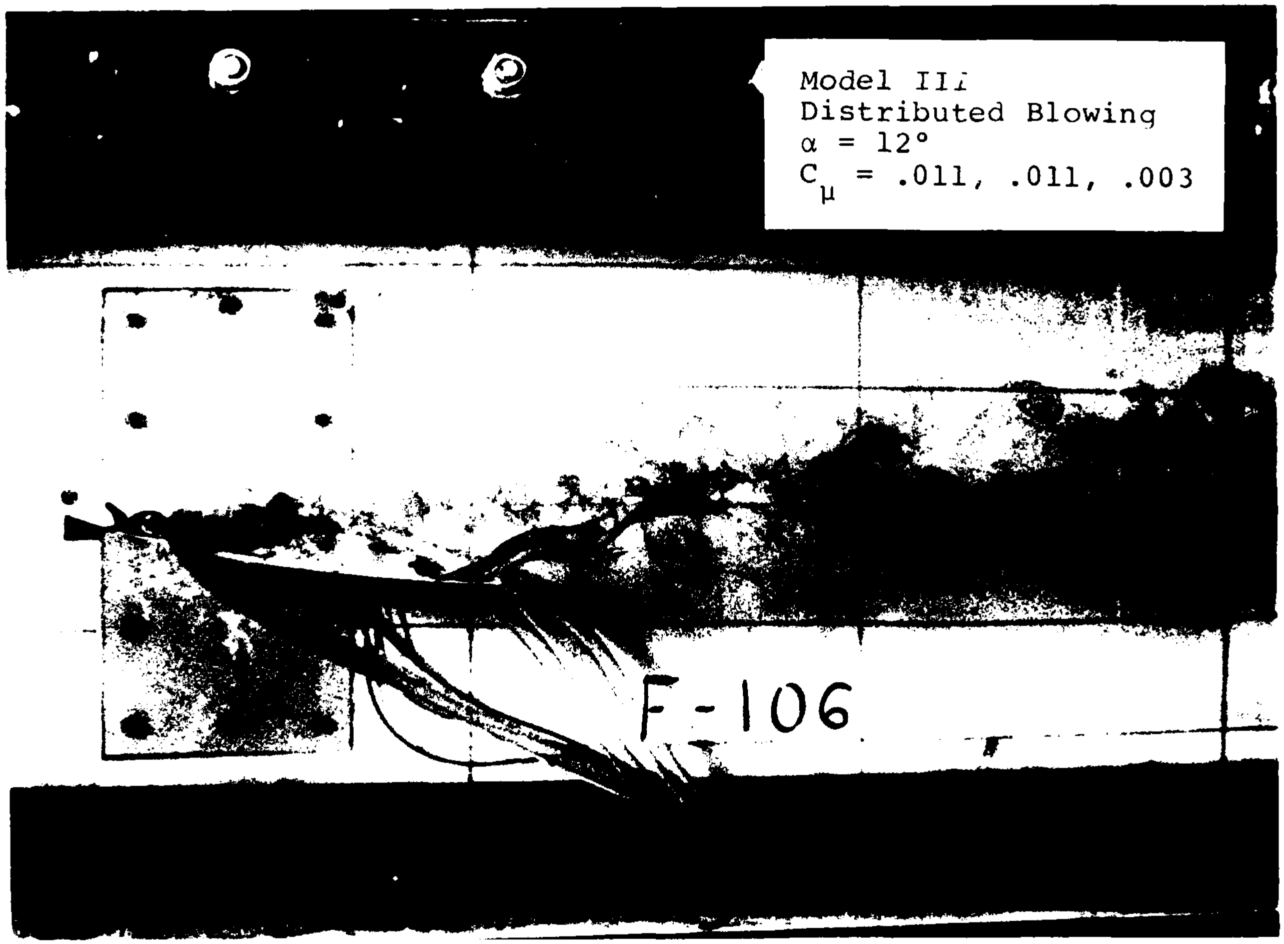

Figure 32. Dispersed Wing Tip Vortex

On Wake Vortex Alleviation

The forward sweep of the front blowing port produced more intense mixing than did blowing from the other ports. The increased mixing could possibly cause one to miss seeing the rotational motion that was present. However, detailed observations of a great many vortex patterns repeatedly showed that distributed blowing which was more concentrated toward the front produced the greatest vortex dispersion. The relationship between the wake disperison and the circulation is unclear at present, and needs to be studied further.

While the degree of observed vortex dispersion is the best measure of the wake vortex alleviation in this type of testing, that criteria is still a subjective one, and it is very difficult to judge the conditions at far downstream. Intense mixing may lessen the observed rotational structure by replacing a strong laminar vortex with an equally strong but undetected turbulent vortex. Secondary vortices of various types may also trigger the Crow instability (Reference 22) and other non-linear multi-vortices interaction instabilities which would cause early destruction of the wake vortices in the far field. These are unknown factors with regard to the wake vortex alleviation, especially in regards to the induced rolling moment to a craft which is behind in a wake flow generated by a larger airplane. Obviously further study is needed as far as the wake vortex hazard is concerned.

5. THEORETICAL ANALYSIS AND COMPUTATIONS

By observing Figure 2 and from the subsequent discussion it can be realized that the flow, field generated by discretely placed jets blowing at the wingtip, is very complicated. Indeed, it was not readily attackable analytically without further understanding the *physics* involved. Nevertheless, in order to obtain some trends of the parameters involved which may guide the direction of future investigations, a simple, three-dimensional vortex lattice method (Reference 16 and 25) was developed and analyzed.

Idealized Model for Analysis

In reality, the discrete jet placed at the wing tip is equivalent to a skewed jet in a non-uniform cross flow. Nevertheless, for the sake of computation, it is a highly idealized case by treating the problem of an individual wingtip jet as a turbulent symmetric jet stream injected into a uniform crossflow stream. It has been reported in numerous observations (e.g., References 26-31), that in general the jet spreads, deforms, deflects and forms a pair of counter rotating vortices after leaving the exit. In turn, the jet interferes with the crossflow to create local blockage, entrainment and wake effect as well. Even though extensive studies have been made on a symmetric jet in a crossflow, the general prediction of flow field is not completely satisfactory. Most of the time, some empiricisms are still incorporated in the solution. Since the main concern in our case was *not* the jet itself but the effect of *jet on* the wing, we chose the simplest way to represent the jet with an approximate model by using the vortex lattice method.

A wing can be represented by a surface network of horse[illegible] tices whose bound vortices coincide with constant percent ch[illegible] along the wing surface. The free portions of vortices aft of th[illegible] edge are assumed to be parallel to the local flow. For simpl[illegible] main wing wake and the tip vortex effects are ignored for the [illegible] ing. The jet blowing from the tip is represented by a curve[illegible] a vortex tube. Following the Monical approach [Ref. 30], th[illegible] assumed to have a square cross section with area equal to th[illegible] the jet exit (i.e., jet port). The last segment of jet is assum[illegible] flared by considering the jet entrainment effect. The angle [illegible] is determined based on the available empirical equations pro[illegible] Monical. The jet is then representable by a flared "jet efflu[illegible] This jet tube is composed of a surface vortex network with th[illegible] lines as the lateral edges. The vortex network is then attach[illegible] tip of the main wing as schematically illustrated in Figure [illegible] constitutes the present model for the analysis.

Margason [Reference 31] has summarized previous studies [illegible] posed an empirical equation to represent the jet centerline tr[illegible] Now, by combining the Monical's jet efflux tube with Margas[illegible] jectory and adapted into a specific geometrical manner at the [illegible] as shown in Figure 34, the jet efflux tube centerline trajector[illegible] described. The jet efflux velocity vector has a combined an[illegible] X-axis and with Y, Z axes as shown. Let x_1, y_1, z_1, be the loc[illegible] sian coordinates parallel to the main wing coordinates x, y, z; [illegible] injected with an angle δ_j with respect to x_1 and with a dihed[illegible] ψ with respect to y_1. The shaded plane as shown in Figure 34

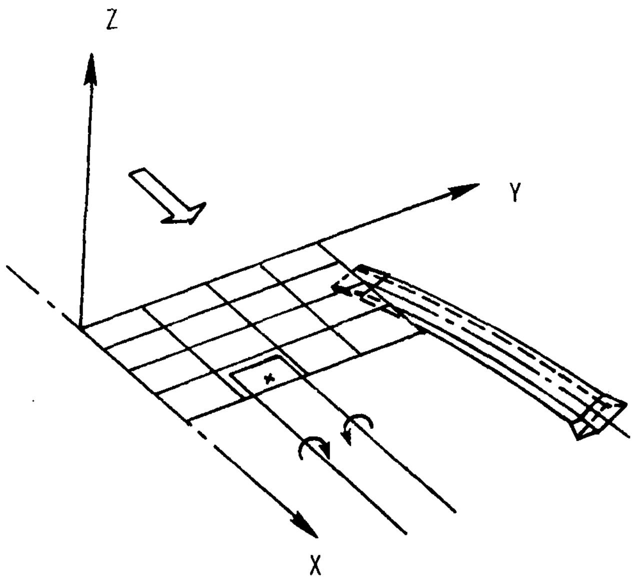

(a) Vortex Lattices Representation of Wing With Jet Efflux Tube Attached.

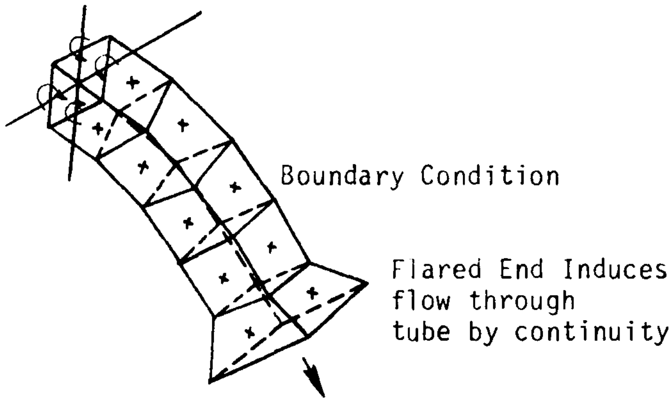

(b) Jet Efflux Tube Modeling

Figure 33. Schematic of Analytical Model.

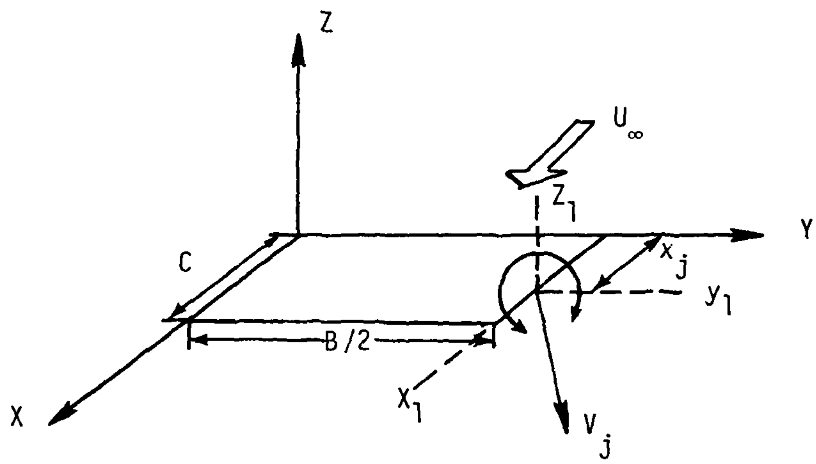

(a) Coordinates for the Wing

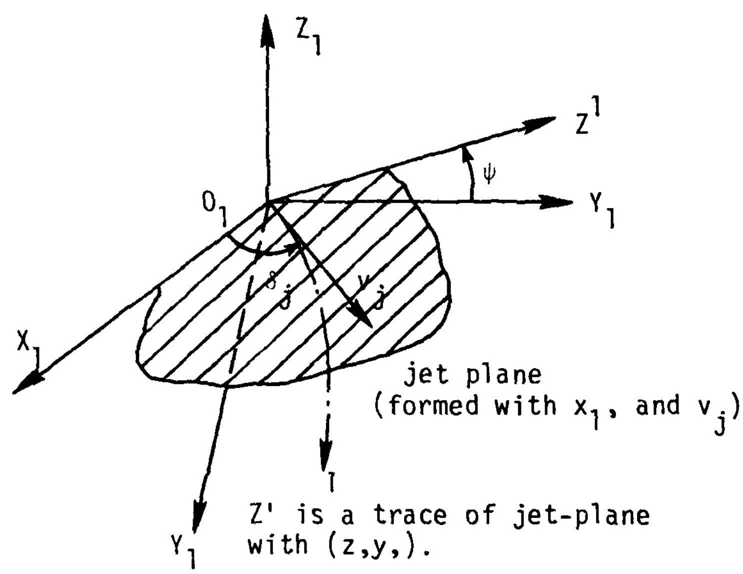

y' perpendicular to jet-plane

jet C.L.

(b) Illustration of Jet Plane

Figure 34. Geometric and Coordinates for Computation

the "jet plane" formed with x_1 and v_1. The new cartesian coordinates x', y', z' can be formed which contain the jet plane. z' is a trace of the jet plane intersect with (z_1, y_1) plane. y' coordinate is perpendicular to the jet plane. In other words, the new coordinates x', y', z' is formed by tilting a plane with ψ angle from y_1 axis and meantime contains the v_j vector which makes δ_j angle with respect to x_1 axis (see Figure 34). Under this consideration, the centerline of jet can be described by the following equation, i.e.,

$$\frac{x'}{d} = \frac{1}{4(v_j/v_\infty)^2 \sin^2 \delta_j} (z'/d)^3 - (z'/d)\, cot\delta_j$$

where x', z' are the jet plane coordinates with the origin coincides with jet port center, d is the equivalent jet diameter, v_j is the jet efflux velocity and v_∞ is the free stream velocity, δ_j is the jet injection angle with respect to the x_1 axis measured in the jet plane. This equation is applied for cases of v_j/v_∞ greater than one.

Procedure for Solution

Set-up of the vortex lattice method for this model is treated in a similar manner as the jet wing case [Reference 25]. The Laplace equation is automatically satisfied in treating this kind of singularity distributions. The control point for each panel of the main wing is located at three quarters of each local chord with individual elementary horseshoe vortices shedding from each surface element. The control points for vortex efflux tube are placed in the center of each elements of the network as shown in Figure 33. The flared end induces flow through the tube by continuity consideration. The boundary conditions on the

wing and on the vortex efflux tube are that the normal velocity at every control point is equal zero. The Kutta condition at the trailing edge of the wing is satisfied by selecting the position of each control point as described.

With these arrangements, the problem is now reduced to solve the linear equations of $N + 4M$ unknown vortex strengths where N is the number of elements on the wing surface and M is the number of elements on each side of vortex tube. These are solved by the Gauss-Seidel iteration scheme. Knowing the vortex strength for each element, the aerodynamic coefficients are calculated by proper integrations.

Discussion on Analytical Results

The analytical model as described above, can treat only one single jet port blowing. Typical results with jet blowing from port I and from port II of tip configuration I are shown in Figure 35. In this figure, the spanwise local normal force coefficients are plotted for with- and-without jet blowing cases. In view of the simplified analytical model, the comparison with measurements are encouraging. The chordwise local loadings are compared in Figure 36. Except at a station very close to the wingtip, the agreements between the measured and computed results are very good. The integrated normal force coefficients with respect to the wing angle of attack are given in Figure 37. In view of wide variations in the jet angles, δ_j and ψ, and different locations of jets, the agreement between the theory and data are again satisfactory.

Based on the present analytical model, several parametric variations were computed. It revealed that our present set up has *not*

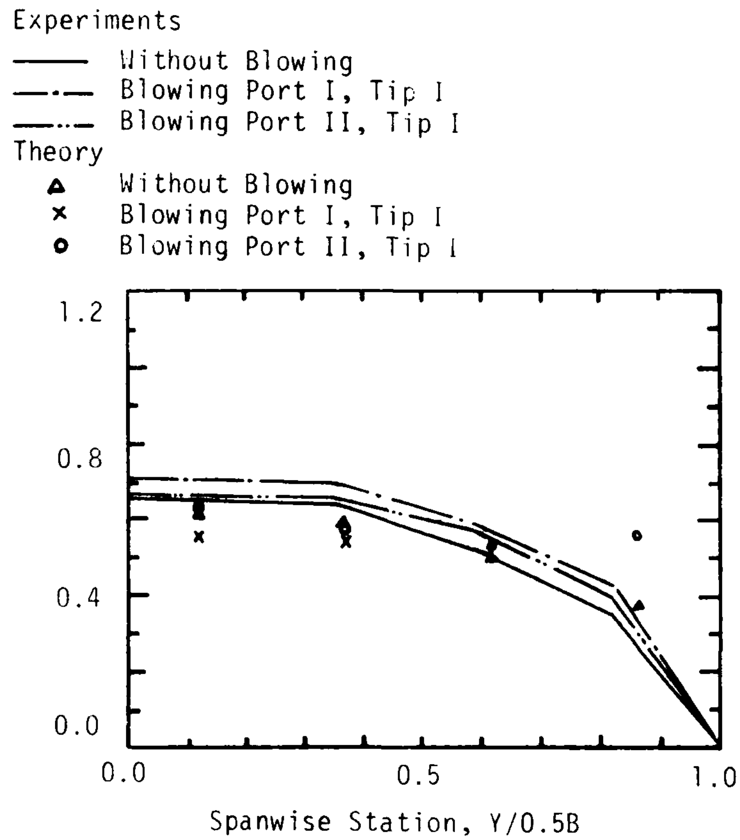

Figure 35. Comparison of Computed Results vs Measurements.

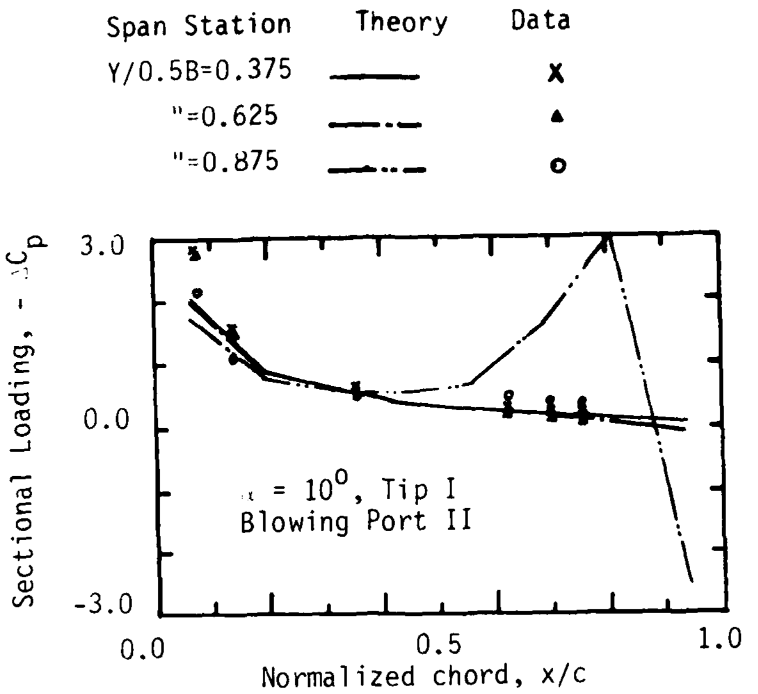

Figure 36. Comparison of Theory vs Measurements on Chordwise Sectional Loading

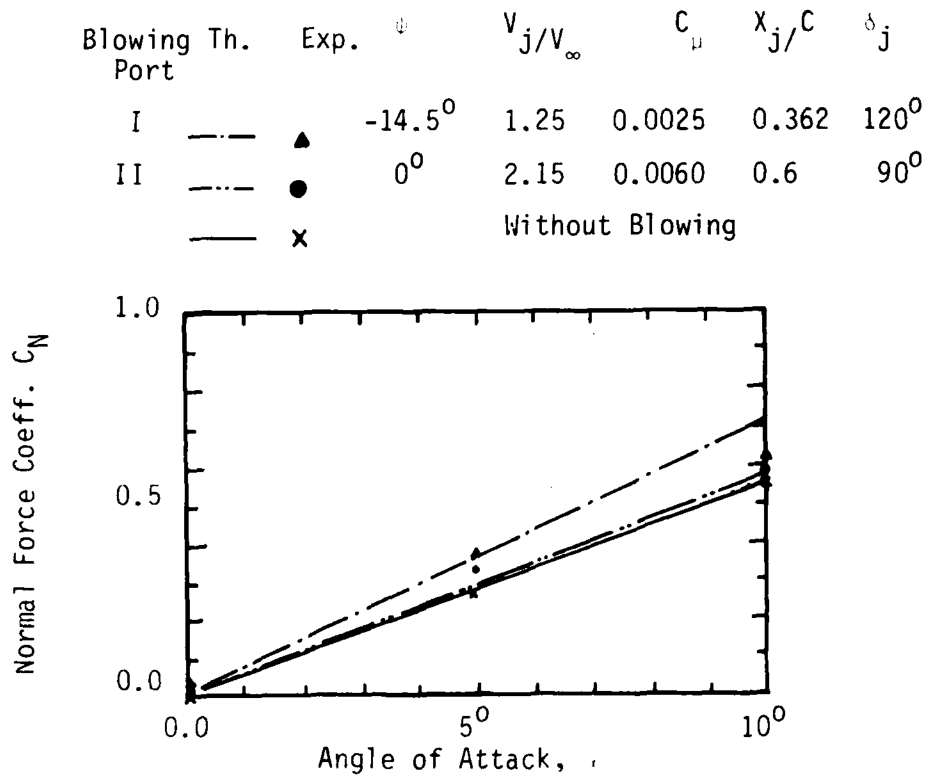

Figure 37. Comparison of Theory and Experiments on Integrated Normal Force Coefficient

reached the maximum potential of improvement on wing performance by the jet blowing. This needs to be further investigated both experimentally and analytically.

6. WAKE VORTEX ROLLUP CALCULATIONS

The vortex trajectory behind the flow field around the wingtip with discrete jets blowing has been computed using a simple mathematical model of wake vortex rollup including some discrete jet effects. The nomenclature and orientation of vortices are illustrated in Figure 38. The model used is a very idealized case. It is two dimensional, inviscid and accounts for jet influence solely by the inclusion of the counter rotating jet vortices (Figure 39). Even though this model appears to be simple, the results are in fundamental agreement with the conclusions drawn from the water tunnel study. The detail description on the computations and the model is given in (Reference 32).

The program used in this calculation was a modified version of a program presented by Chow (Reference 33). One improvement to the wing vortex model developed by Chow was in the original locations of the discrete vortices. The vortex sheet is divided into a number of spanwise intervals, and in the original program a discrete vortex with the total strength of the sheet over that interval is located at the center of the interval. Since the sheet strength $\gamma(y)$ is not constant, the vortices within an interval would induce a velocity at the center of the interval. This self-induced velocity was neglected by Chow, but he pointed out that more realistic results could be attained by placing the discrete vortex at the point in the interval where the self induced velocity should be zero. This was done and helped to delay the occurrence of chaotic motion which Chow found in the tip region at large $T(T = t\Gamma_0/2\pi a^2$, where Γ_0 is the circulation in the plane of symmetry of an elliptically

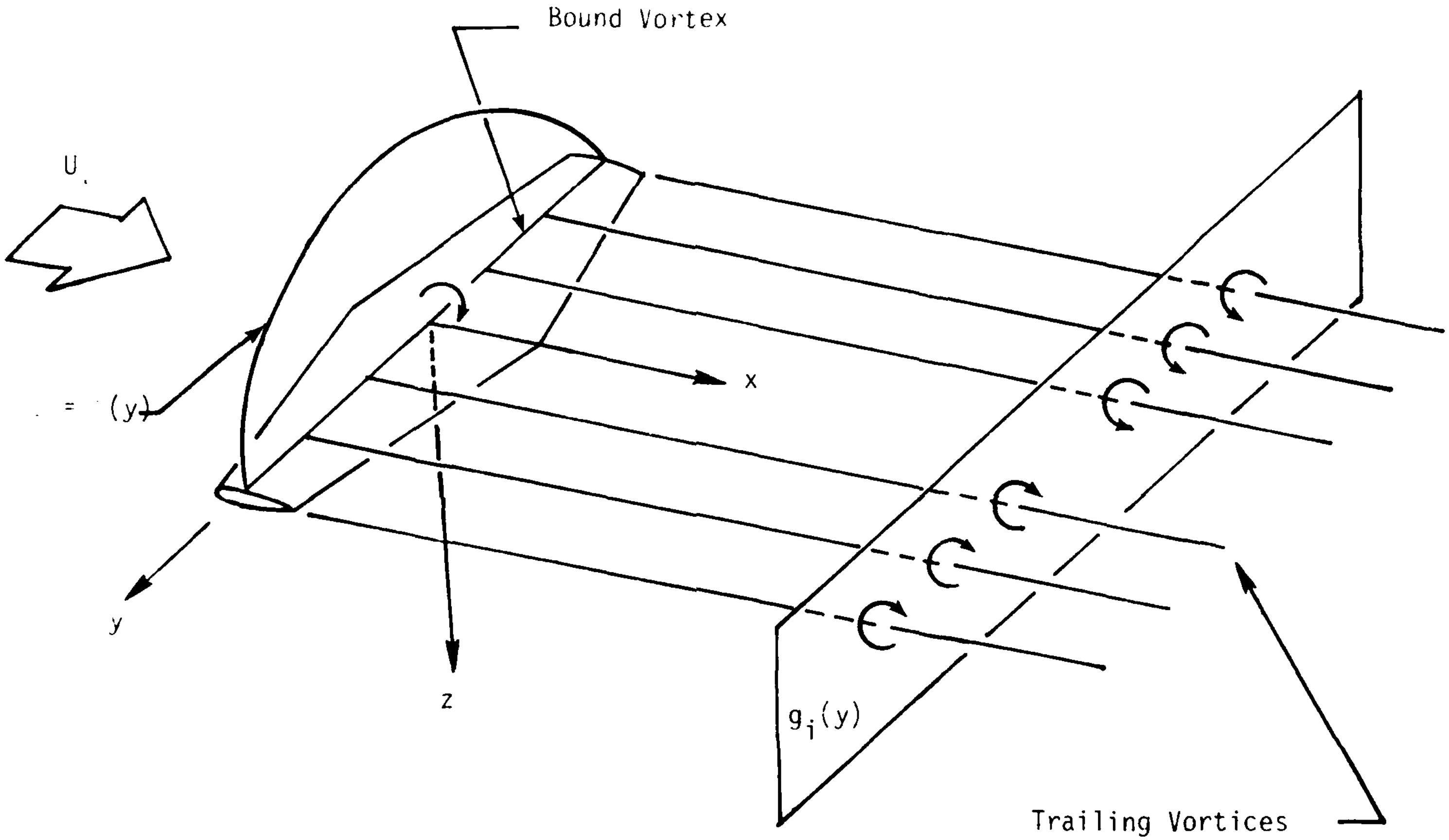

Figure 38. Three-Dimensional Wing and Wake Model.

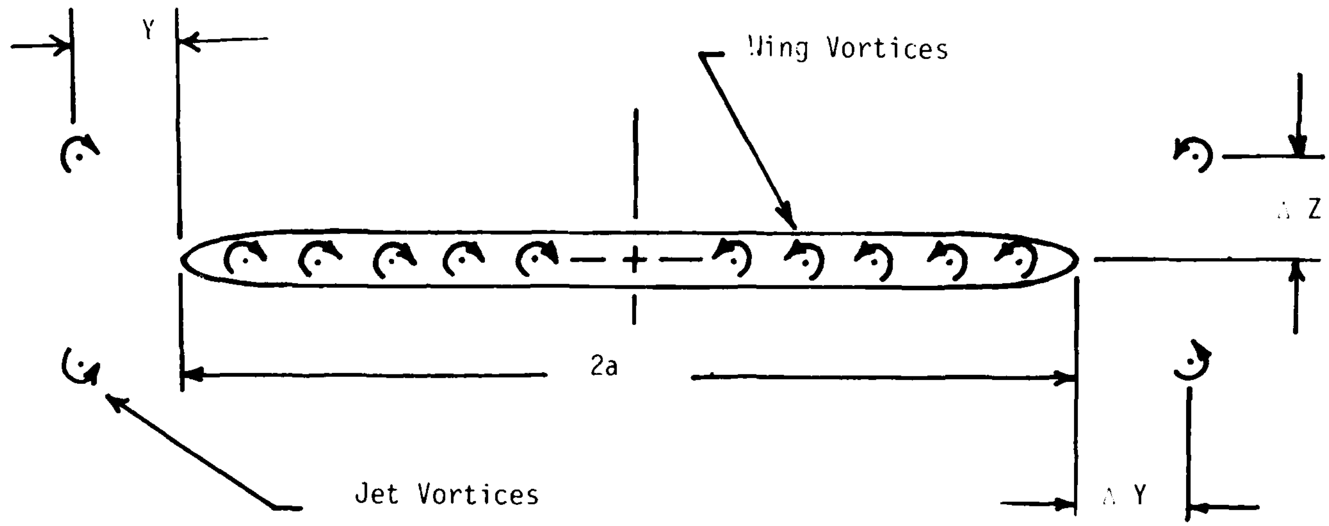

Wake Vortex Roll Up Study With Tow Counter Rotating Pair of Vortices Placed Near The Wing Tip (Note: Small Distances of ΔZ and ΔY)

Figure 39.

loaded wing). However, even better results were obtained by originally placing the vortices at the centroid of vorticity over the interval they represent as had been done by Moore (Reference 34) and by Clements and Maull (Reference 35). Consequently, this method was used in all calculations. The major improvement to the program was the incorporation of Moore's criteria for the merging of vortices in the wing tip spiral. This modification completely prevented chaotic motion in the tip region. Other improvements included the use of double precision arithmetic and an option to discretize the system with vortices of equal strength as opposed to intervals of equal spacing that contained vortices of variable strengths. The program was run with no discrete jet influences and checked almost identically with Moore's results.

The goal of this computational investigation was to better understand the effect of the discrete jets and to verify flow patterns seen in the water tunnel.

Jet Vortices Near the Wingtip

The dominant influence of the wing tip jets, especially outside the immediate vicinity of the jet prot, is the set of counter rotating vortices which are produced (e.g., jet in cross flow, References 36-38). To model this influence a pair of two-dimensional counter rotating vortices was placed outboard of each wing tip with a distance of ΔY and ΔZ away from the wing as shown in Figure 39. The strength of these vortices varied according to the data presented by Krausche, Fearn, and Weston (Reference 38) for a jet ejecting at 90 degrees to the freestream. Decreases in strength due to diffusion were included in the math model and the two levels of blowing for which data was available $R = Vj/V\infty$ =

4 and 8 were both used. These jet velocity ratios equate to very reasonable jet coefficients. For single port blowing from the water tunnel model, velocity ratios of 4 and 8 give jet coefficients of $C_\mu = 0.012$ and 0.047. These jet coefficients represent moderate blowing in the water tunnel. No attempt was made to simulate multiple port blowing in this two-dimensional model.

The output of the program was the change in the rollup of the wing vortices due to the effects of the jet vortices. However, the jet vortices also moved due to the influence of each other and the wing vortex system. Their trajectories were output and proved to be very useful in analyzing the results.

Figure 40 is a comparison of the wake vortex rollup pattern at $T = 0.15$ (a baseline time, corresponding to approximately 5 chord length behind the wing) with and without a pair of vortices placed at $\Delta Y = 0.05$ and $\Delta Z = 0.10$. Jet vortices are originally located at the baseline position. As can be seen, the vortex sheet of the wing with no jet influences has rolled up into the nice spiral found in earlier work. On the other hand, the wing with the jet vortices included has rolled up into a spiral that is less well defined with uneven spacing between vortices in the tip region. This lack of definition is due to numerous vortices being combined in the tip region according to Moore's criteria. Despite the lack of detail for the second spiral, several key results are immediately obvious in this plot (Figure 40). First, the jet has caused the vortex core to be shifted upwards significantly. Comparing the last vortex in each line shows that the up-shift caused by the jet is greater than 20 percent of the wing semispan. This is a very sizable

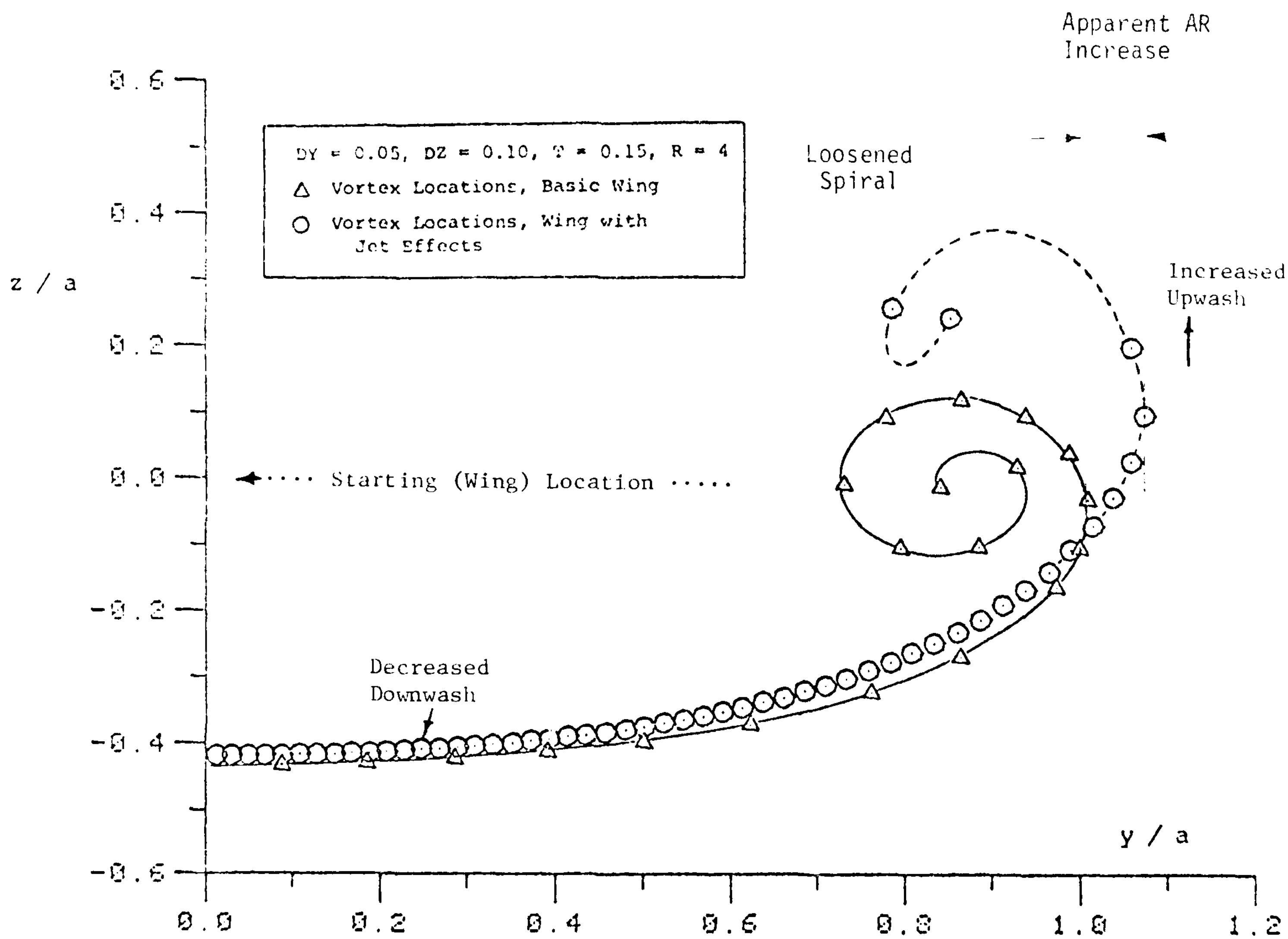

Figure 40. Wake Vortex Roll Up with Symmetric Vortices Jet Effects.

shift and agrees favorably with the similar shift seen in severa
water tunnel tests. Second, one sees that the interior vortices
wing vortex system with jet effects included have not moved d
much as those in the basic wing (a reduction in the downwash
evident). Third, the wake vortex roll-up is significantly reduc
the presence of a pair of vortices by the jet. Following Moore (Re
33), the rolled up portion of the sheet is defined as the part b
the center of the spiral and the point where the tangent is last
to the z axis. Performing this comparison one finds that the tip
for the basic wing contains 71.4% of the total vorticity on the se
while the vortex for the wing with jets contains <u>only</u> 57.7% of th
vorticity (a clear reduction in the tip vortex strength). Fourth th
flow is extended approximately 8% beyond th extent of span (
evidence of increasing its "apparent aspect ratio". All of these
agree with the water tunnel observations.

Figure 41 is a plot of the same data seen in Figure 40, b
trajectory of the counterrotating vortex pair has been added
upper vortex which rotates similar to the wing vortex system b
entangled in the rolling up vortex sheet and would probably not
as a separate flow structure in the water tunnel. The lower
which rotates opposite to all the others vortices, rotates arou
system exactly as was <u>seen</u> in many water tunnel observations v
port jet blowing. This counter rotating vortex is very likely the s
"auxiliary vortex" seen and discussed in the water tunnel observ

The lack of detail on the rolled up vortex as shown in Fig
and 41 is typical of those cases where the jet caused significant

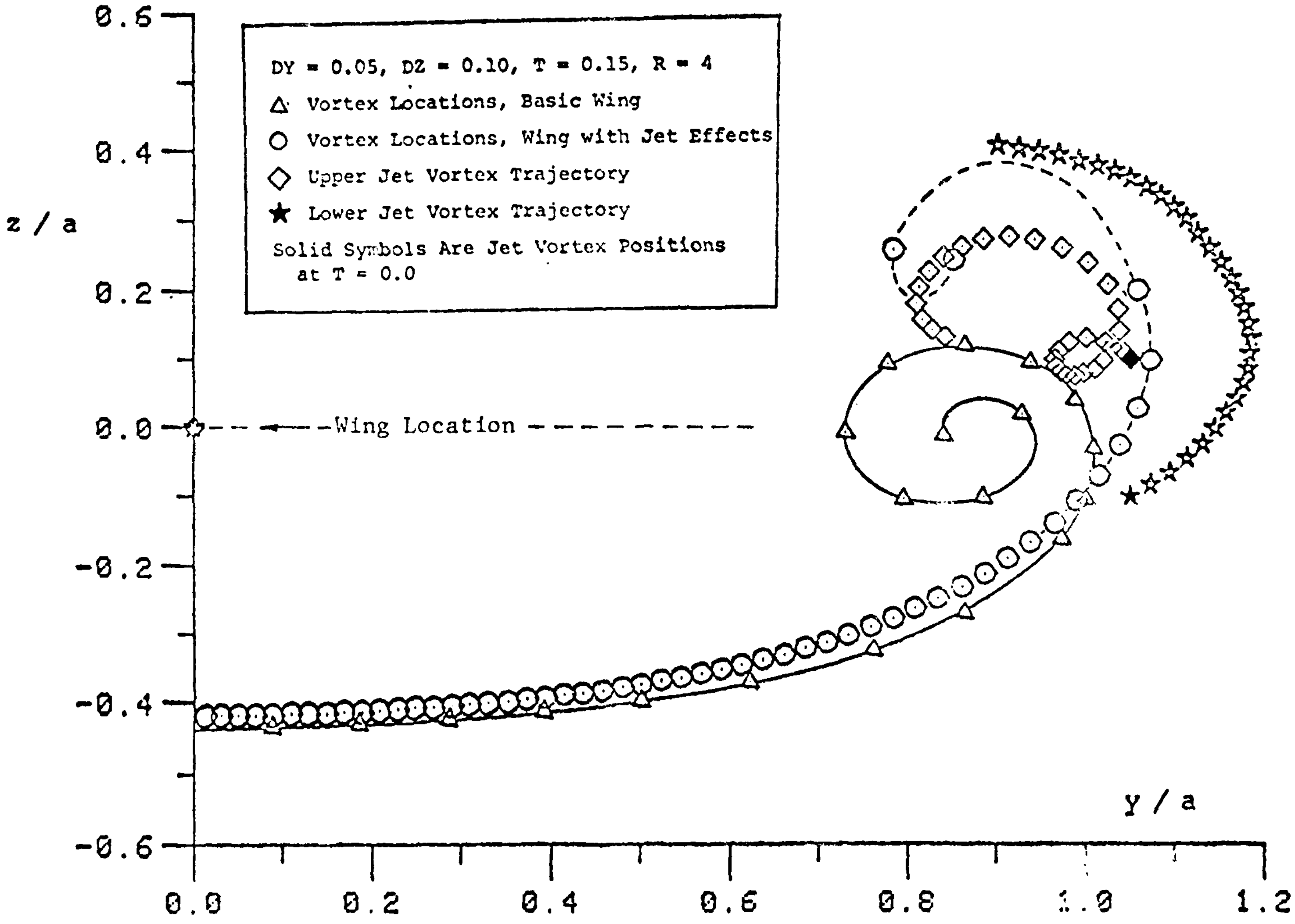

Figure 41. Trajectories of A Pair of Jet Vortices Due to Interactions

shift and/or substantial reduction in rolled up vortex strength. In those cases where the jet vortices were less effective the resulting roll up was defined much better. For example, Figure 42 compares the basic wing roll up with the roll up for jet vortices initially at DY = 0.15 and DZ = 0.10. Both vortex sheets form a very nice spiral, and the core of the jet modified vortex is elevated much less than was seen in Figure 40. The strength of the jet modified vortex is 64.2% of the total vorticity for this case. The decline in jet effectiveness is due to the jet vortices originally being located further outboard than was used earlier.

As would be expected, the decrease in downwash achieved by the jets can be enhanced by increasing vorticity in the counterrotating element of vortices which rotates opposite to the wing system. Figure 43 points this out very dramatically. The jet vortex which rotates similarly to the wing vortex system has been eliminated (a limiting case) and the downwash as measured by the travel of vortices near the plane of symmetry is greatly reduced. This downwash reduction would be beneficial to the wing aerodynamic performance. In our wind and water tunnel experiments, the jet orientation was skewed with respect to the local cross flow. Thus, in reality, the experimental results should lie in between the case of a symmetric pair of vortices and the limiting case of only one counter rotating (lower) vortex as explained above. In practice, there are a few techniques to enhance the counterrotating jet vortex by including triangular or other nonsymmetric jet ports and or imposed rotation on the jet fluid prior to ejection.

Effect of Jet Vortex Initial Location

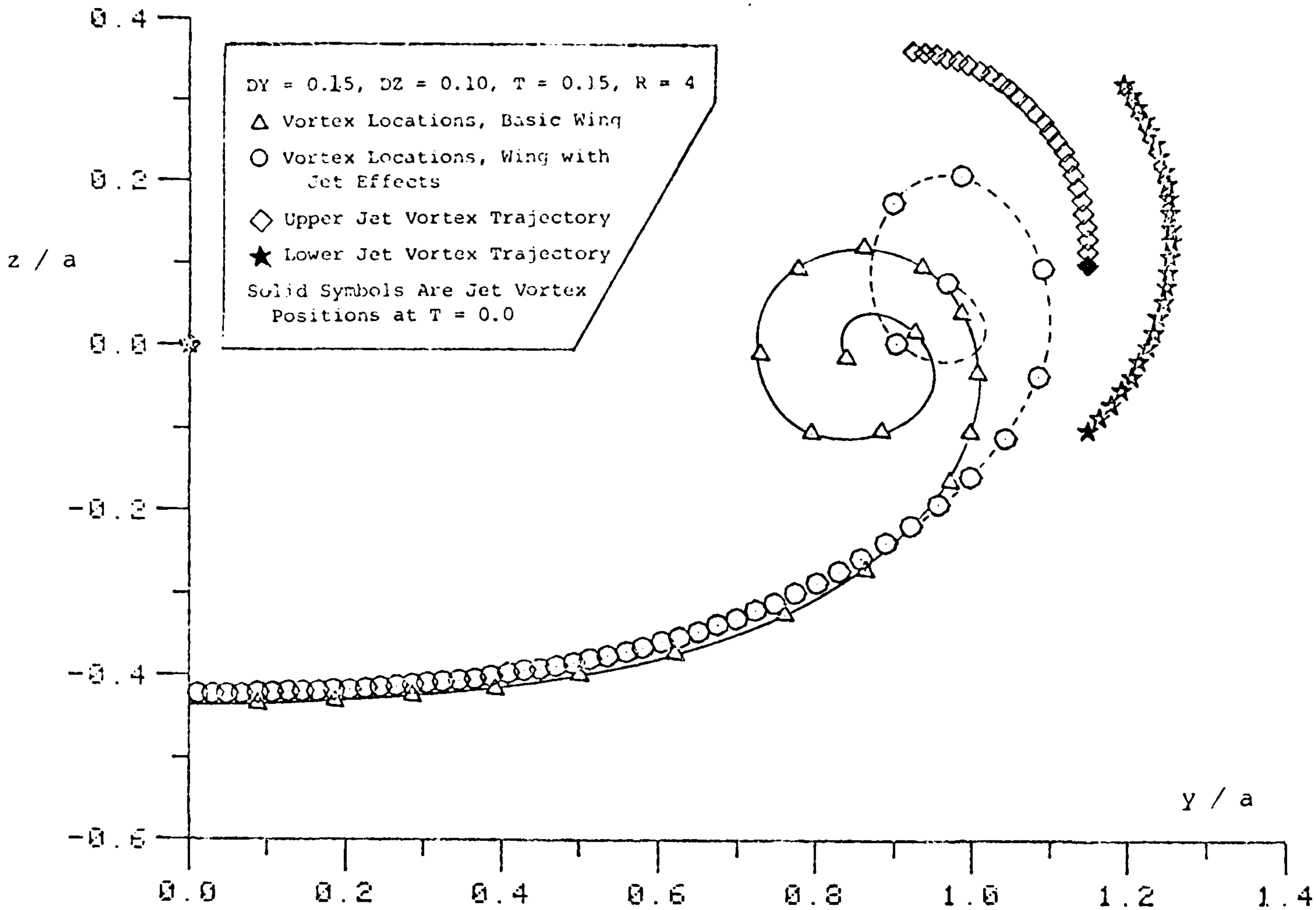

Figure 42. Roll Up with Jets Far Outboard

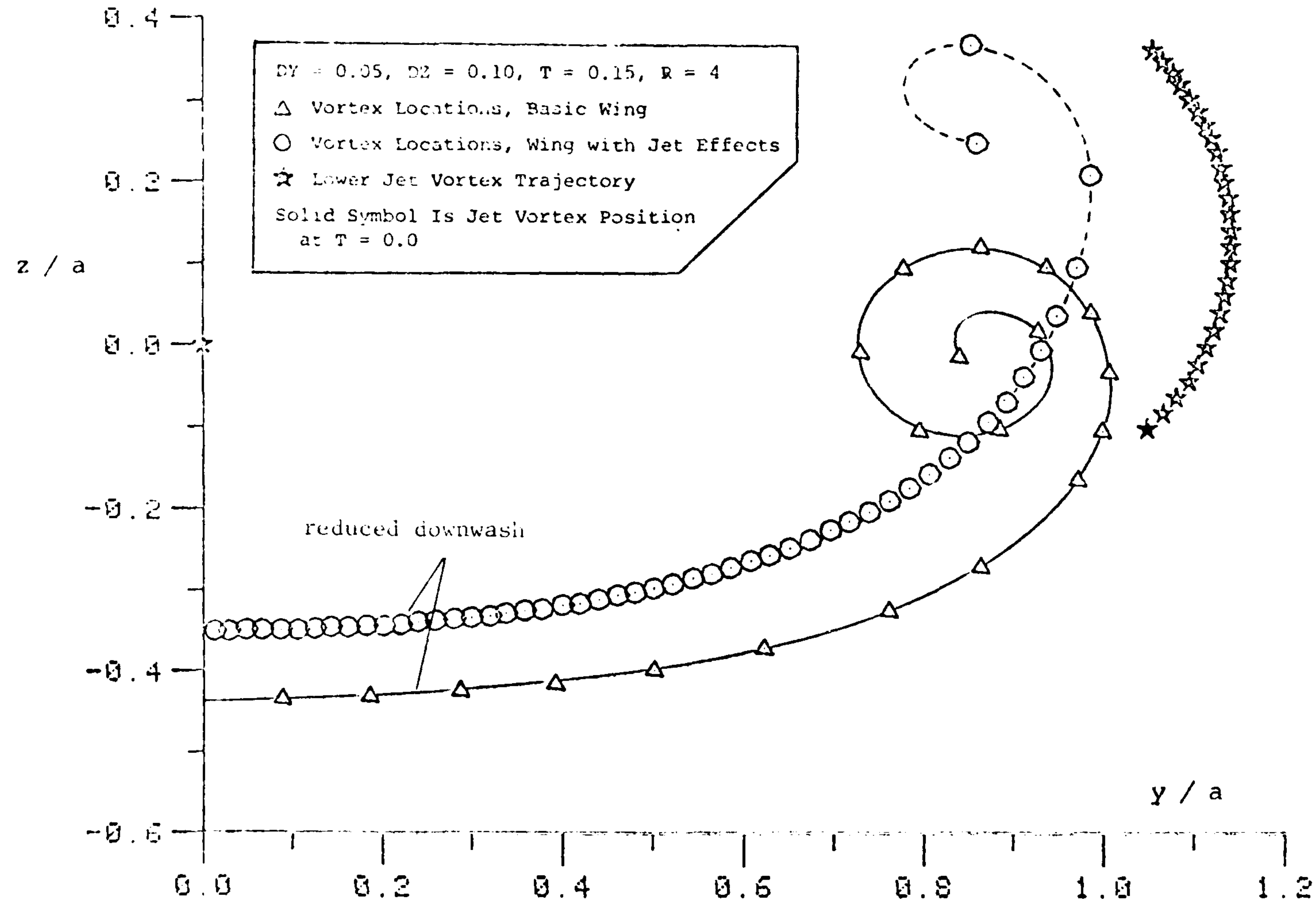

Figure 43. Roll Up with Unsymmetric Jet Vortices

The initial location of the counterrotating vortex pair strongly affects their trajectory and interaction with the wing tip vortex. As seen earlier, an extreme outboard location (DY = 0.15) causes the vortex pair to rotate around the tip vortex but to be too far removed from it to be effective. This was also seen in the water tunnel experiments.

Other influences of location were also found to occur. Figures 44 and 45 summarize the influence of initial jet vortex position on the strength of the rolled up portion of the wing tip vortex. Also shown is the rolled up vortex strength for no jet blowing. One immediate observation is that the jet vortices have a favorable influence on alleviating the rolled up strength wherever they originate. This was almost universally true; only some locations where the counterrotating vortices were inboard of the tip (an unrealistic situation) showed no increase in wing tip vortex strength.

The optimum position, however, for the counterrotating vortices to originate is near the selected baseline conditions (DY = 0.05, DZ = 0.10). Additionally, the rolled up strength is apparently more sensitive to the vertical spacing between the vortices (DZ) than it is to the distance of the vortices from the wing tip. This is especially true as the counterrotating vortices closely approach each other. The reason for this can be seen in Figure 46 where DY = 0.05 and DZ = 0.025. In this case the influence of each vortex in the counterrotating pair is concentrated on the other member. Thus the pair moves together very rapidly out of the roll up region completely. At some point they approach each other so closely that they cross; at this point the model would be invalid since viscous effects would become very important as

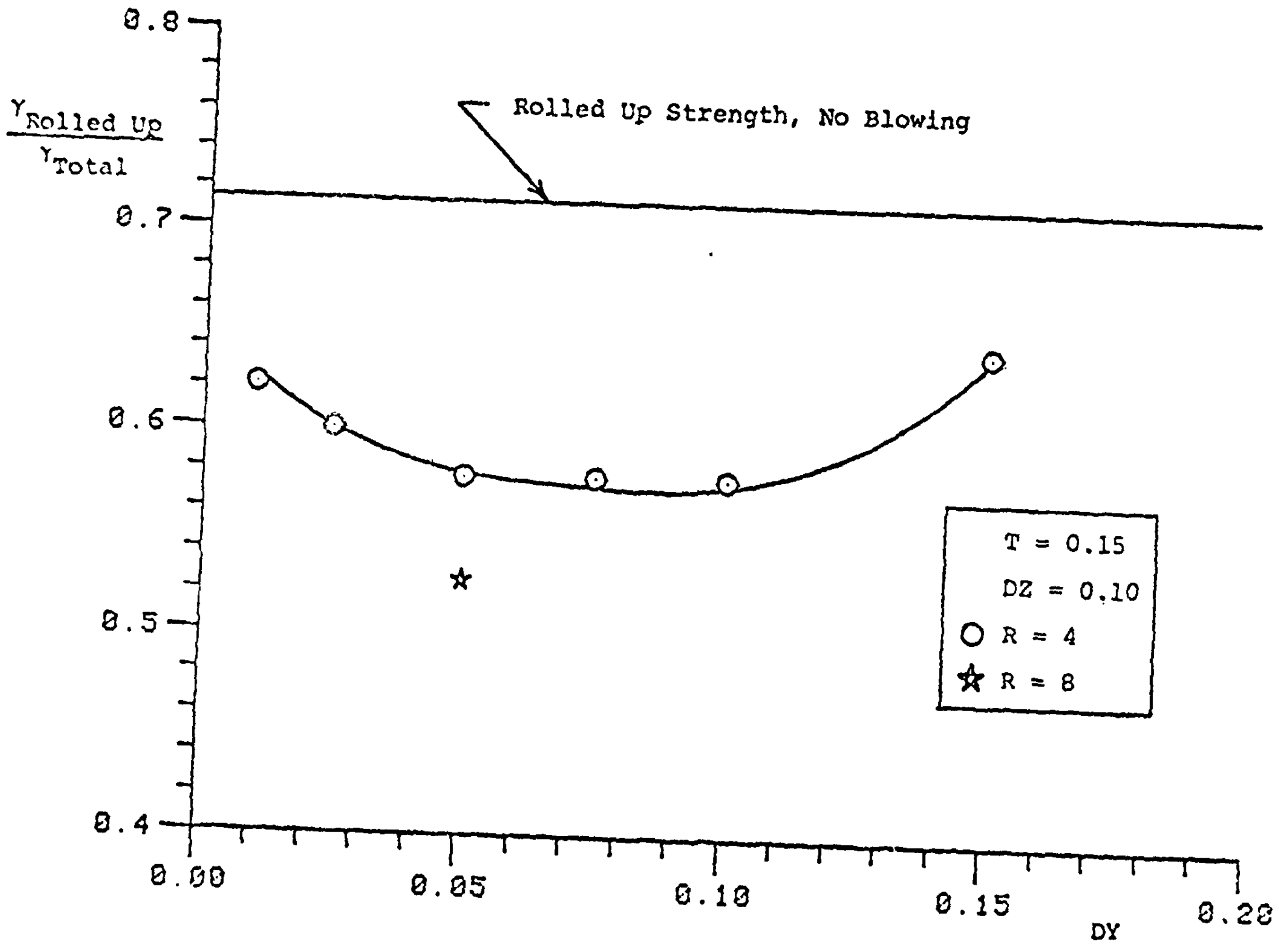

Figure 44. Effect of Spanwise Spacing on Rolled Up Strength

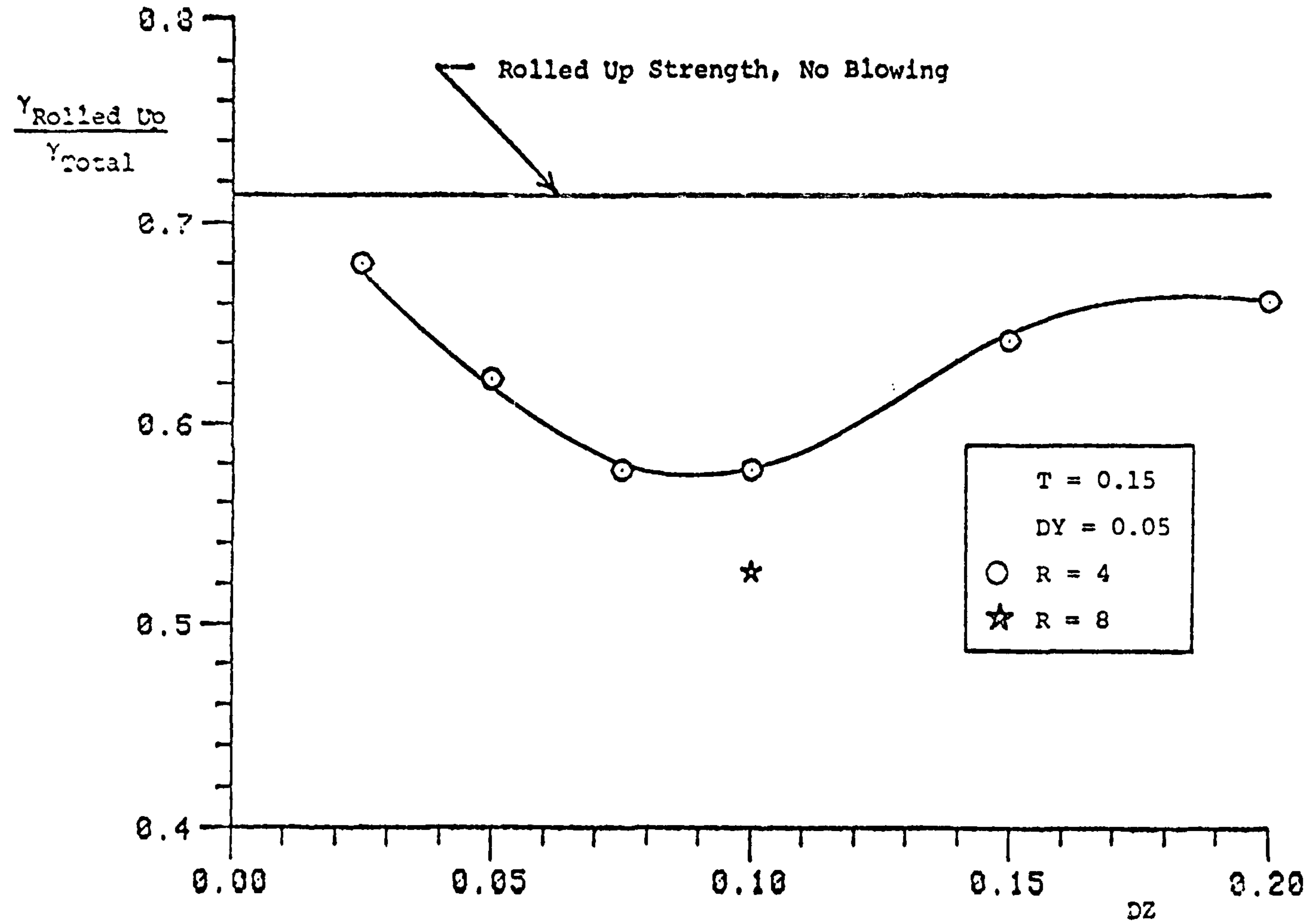

Figure 45. Effect of Vertical Spacing on Rolled Up Strength

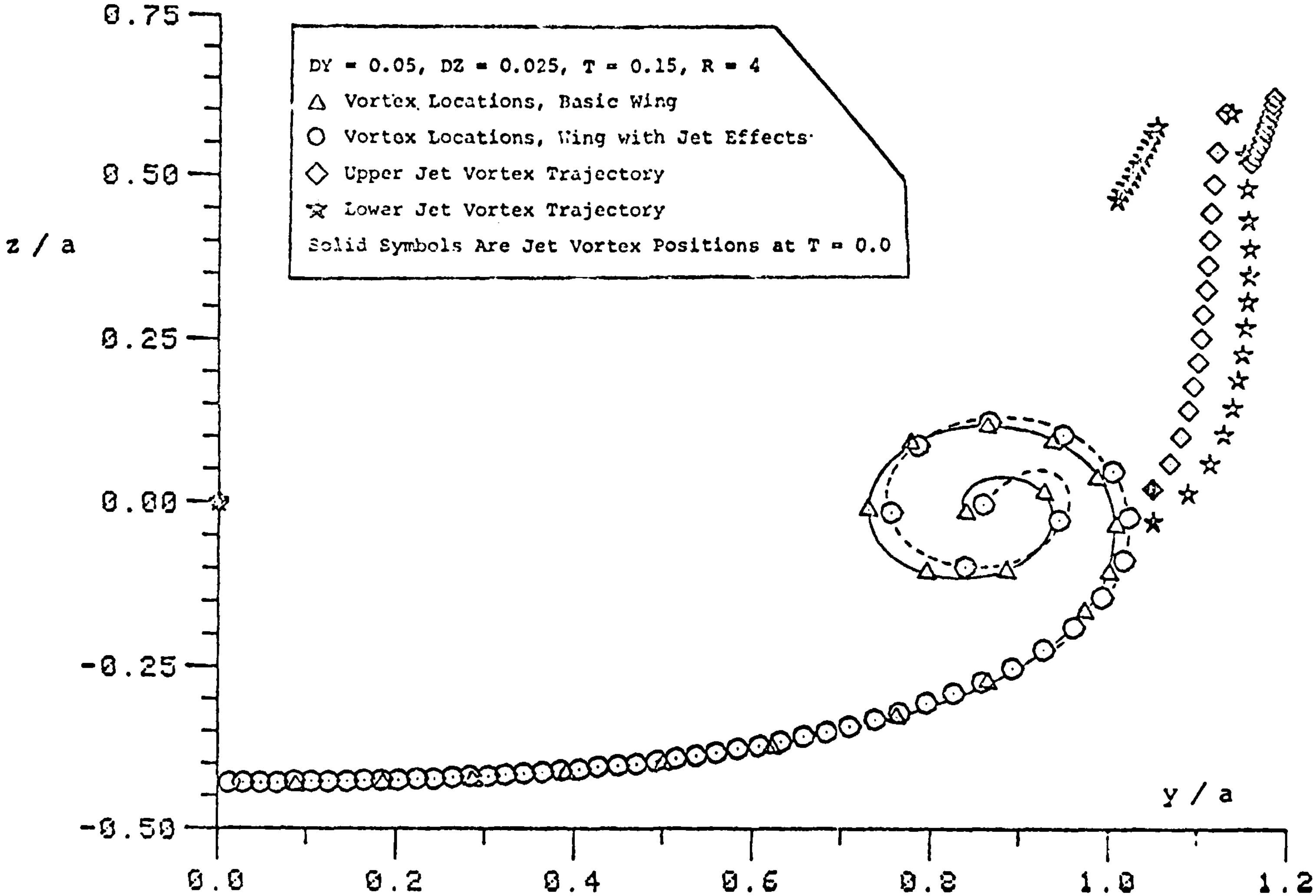

Figure 46. Roll Up with Paired Drifting of Jet Vortices

well as the nonlinear vortex interactions. This two-dimensional calculation probably overpredicts the movement of the vortices with respect to the three-dimensional case. In the real flow field, the momentum of the crossflow would exert a strong influence on the jet vortex trajectories and probably prevent, or at lest retard, this type of paired drifting. Yet, the model does point out the importance of interacting the jet vortices with the wing vortex system rather than with each other.

The initial position of the jet vortices also has a significant impact on the amount of stretching that is done on the wing vortex sheet. If DY is small and DZ is also small, but above the level where the paired influences dominate, this stretching can be quite large. Figure 47 compares the initial roll up of the basic wing with that of a jet equipped wing with the initial jet vortices at DZ = 0.025 and DY = 0.025, at T = 0.005. The basic wing vortex has already rolled up in the first spiral while the jet equipped wing vortex is still stretching. This indicates the significance of jet singularities at early stages of the wake vortex development.

It is also interesting to note that the jet vortices in Figure 47b did not pair off and move out of the roll up region even though they were as close originally as those shown in Figure 46. Obviously the position with respect to the wing tip is also important in controlling the degree of interaction between the jet vortices and the wing tip vortex

The importance of initial jet vortex position is clear, but controlling the initial position must be possible in order to take advantage of the lessons learned. Some control of trajectory was noted in the experimental part of this investigation, but no control of the vertical

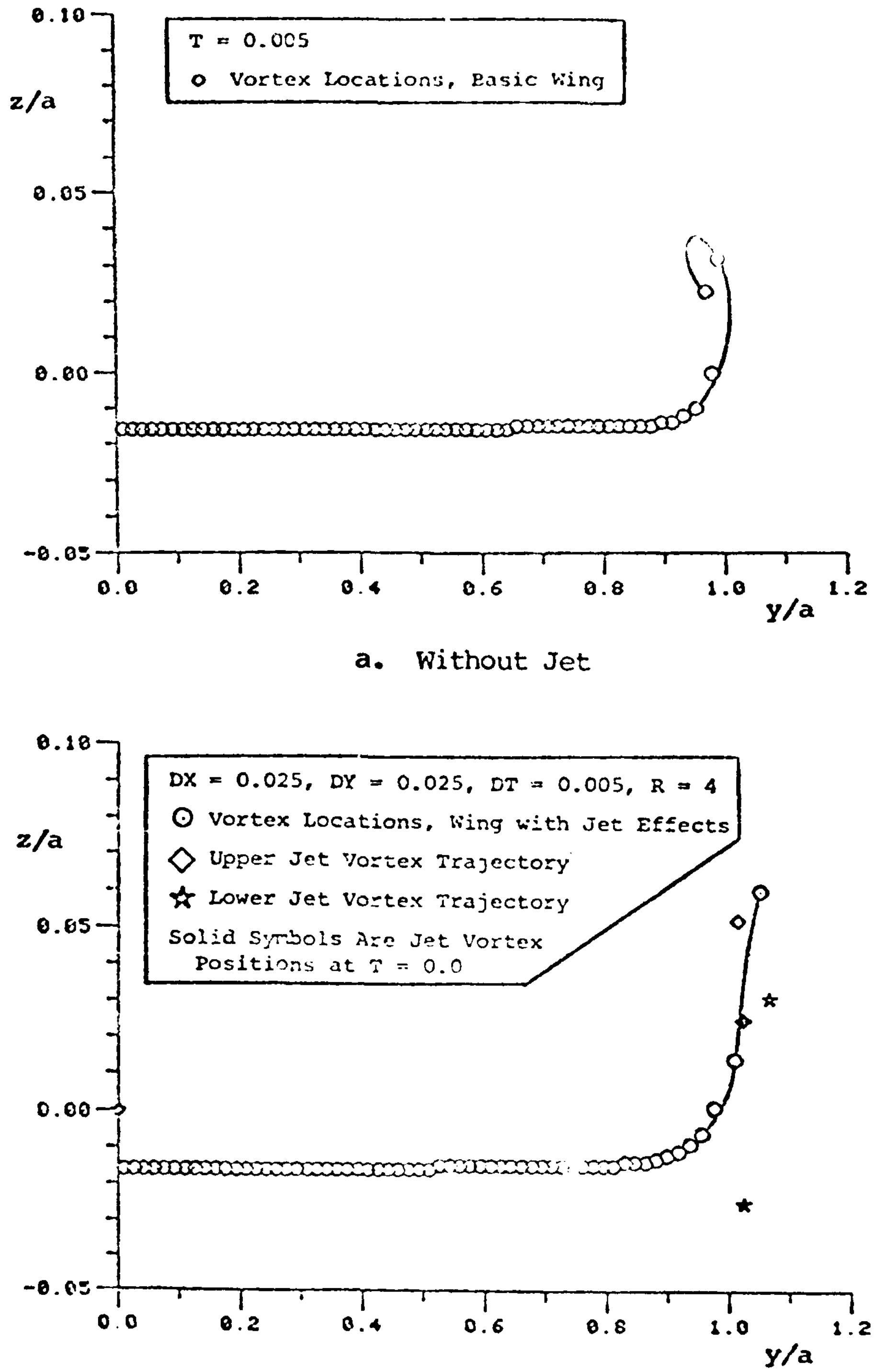

Figure 47. Importance of the 'Initial' Singularity Effect

spacing, DZ, was either attempted or observed. Fortunately, the data of Krausche Fearn and Weston (Reference 38) show that vertical spacing is a function of jet injection angle. This influence should be considered in the design of future jet ports.

Effect of Jet Vortex Strength

The effect of increasing jet vortex strength is to increase the elevation of the vortex core and to decrease the strength of the rolled up wing tip vortex. Figures 44 and 45 presented the rolled up strength for jet vortices with a jet velocity ratio, $R = V_j/V_\infty = 8$, and located at the baseline position. The strength was 52.6% from the strength of the total vorticity which is a reduction of 26.3% from the strength of the no jet rolled up vortex. Higher jet vortex strength also magnifies the stretching of the wing vortex sheet which was described previously.

7. CONCLUSIONS

Based on a totally new concept of discrete blowing jets from the wing tip, we have obtained significant results as outlined below:

1. With relatively low jet C_μ $(0.001 < C_\mu < 0.01)$ significant change in the pressure distribution on both the upper and the lower wing surfaces were observed. The jets effect was not a localized phenomenon but it resulted in an overall influence. This result suggested that the total "wing circulation" had been altered due to small amount of jet blowing in the wind tunnel experiments. This was evidenced in the pressure data plots both in the chordwise and the spanwise directions. The resulting modification of tip flow field had a significant effect on the wing loading.

2. Three completely different and independent types of secondary vortices were generated with wingtip jet blowing in the water tunnel flow visualization experiments. They are:

   (i) Periodic, perpendicular to the main flow "Spin-off" vortices which extended far into the potential flow region. The production of this type of secondary vortices is attributed to the local nonsteadiness induced by the jet blowing.

   (ii) Counter-rotating "Auxiliary vortices", were nearly parallel to the main flow, and interacted strongly with the wingtip vortex flow. The secondary vortex of this type is attributed to the skewed jet in a cross flow.

(iii) Periodic, "Entrained vortices" connected the jet vortex and the wingtip vortex. These were much weaker secondary vortices attributed to the entrainment effect by the jet.

3. Two analytical models were developed to compute the flow field around the wing-tip and to predict the wing loading with the wing-tip jets. Reasonable agreement with the experimental observations were found.

As a consequence of the above combined phenomena, the tip wake flow was moved outboard and upward, the wake vortex was significantly dispersed, and meantime, its total circulation increased. The increase in the "apparent aspect ratio" due to jet was evident and large. The increased circulation on the wake flow was responsible for the wing performance improvement.

To the best of our knowledge, no literature has reported similar findings. Therefore, we support the notion that applying jets discretely at the wingtip is indeed a novel and very original idea toward utilizing local interacting flow field for the improvement of overall wing performance. Further detail study is much needed to fundamentally understand the complicated three dimensional interacting flow field. If properly designed, the discrete wingtip jets promise to be a viable technique for improving wing performance.

AD-A148 981 AERODYNAMIC IMPROVEMENTS BY DISCRETE WING TIP JETS(U) 2/2
TENNESSEE UNIV SPACE INST TULLAHOMA GASDYNAMICS DIV
J M WU ET AL. MAR 84 AFWAL-TR-84-3009 F33615-81-K-3034

UNCLASSIFIED F/G 20/4 NL

END

FILMED

DTIC

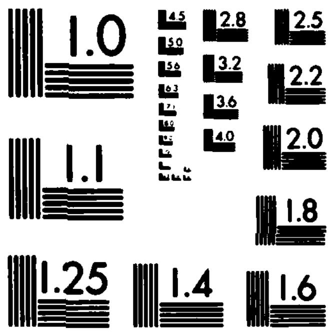

MICROCOPY RESOLUTION TEST CHART
NATIONAL BUREAU OF STANDARDS-1963-A

REFERENCES

1. Whitcomb, R. T., "A Design Approach and Selected Wind-Tunnel Results at High Subsonic Speeds for Wing-Tip Mounted Winglets," NASA Tnd-8260, 1976.

2. Munk, Max M., "The Minimum Induced Drag of Airfoils," NACA Report No. 12, 1921.

3. Reid, E. G., "The Effects of Shielding the Tips of Airfoils," NACA TR 201, Langley Memorial Aeronautical Laboratory, Langley Field. Virginia 1925.

4. Hemke, P. E., "Drag of Wings with End Plates," NACATR 267, Langley Memorial Aeronautical Laboratory, Langley Field, Virginia, January, 1927.

5. Von Karman, T. and Burgers, J. M., "General Aerodynamic Theory-Perfect Fluid," Aerodynamic Theory, Durand, W. F., Editor. Div. E., Vol. I Berlin/Vienna: Julins Spring-Verlang, pp. 316-321, 1934-1036, and New York: Dover Publications, Inc., pp. 216-221, 1963.

6. Mangler, W., "The Lift Distribution of Wings with End Plates," NACATM 856, Translated by Vanier, J., Luftfahrt Forschung, 14 (No. 11): 564-569, November 20, 1937.

7. Mangler, W., "Die Auftriebsverteilung am Tragflugel mit Sitlichen Scheiben," Luftfahrt-Forschung, 14 (No. 5): 219-228, May, 1939.

8. Reiba, J. M. and Watson, J. M., "The Effect of End Plates on Swept Wings at Low Speed," NACA TN 2229, Langley Aeronautical Laboratory, Langley Field, Virginia, August, 1951.

9. Riley, D. R., "Wind-Tunnel Investigation and Analysis of the Effects of End Plates on the Aerodynamic Characteristics of an Unswept Wing," NACA TN 2440, Langley Aeronautical Laboratory, Langley Field, Virginia, August, 1951.

10. Clements, J. R., "Canted Adjustable End Plates for the Control of Drag," Aeronautical Engineering Review, 14:40-44, July, 1955.

11. Weber, J., "Theoretical Load Distribution On a Wing with Vertical Plates," British A.R.C. R & M 2960, March, 1956.

12. Cone, C. D., Jr., "The Theory of Induced Lift and Minimum Induced Drag of Nonplanar Liftinng Systems," NASATRR-139, Langley Research Center, Langley Station, Hampton, Virginia, February, 1962.

13. Lundry, J. L., and Lissaman, P. B., "A Numerical Solution for the Minimum Induced Drag of Nonplanar Wings," Journal of Aircraft, 5:12-21, January-February, 1968.

14. See Witcomb, R. T. Ref. 1 and its application to various aircrafts on CTOL Conference Report, NASA Langley Research Center, Feb. 28-March 3, 1978, Hampton, Virginia.

15. Flechner, S. G., Jacobs, P. F., and Whitcomb, R. T., "A High Sub-

sonic Speed Windtunnel Investigation of Winglets on a Representative Second-Generation Jet Transport Wing," NASATnd-8264, 1976.

16. Wu, J. M., A. Vakili, and Z. L. Chen, "Wing-Tip Jets Aerodynamic Performance," Proceedings of the 13th International Council for Aeronautical Sciences, Ed. B. Laschka and R. Staufenbiel, Seattle, Washington, August, 1982.

17. Wu, J. M., A. Vakili. Z. L. Chen and F. T. Gilliam, "Investigation on the Effects of Discrete Wingtip Jets," AIAA paper No. 83-0546, AIAA 21st Aerospace Sciences Meeting, Reno,, Nevada, January, 1963.

18. Lloyd, A., "The Effects of Spanwise Blowing On the Aerodynamic Characteristics of a Low Aspect Ratio Wing," Von Karman Institute Project Report 1963-90. Rhode-st. Geneses, Belgium, 1963.

19. Carafoli, F. and Camarasescu, N., "New Researchers on Small Span-Chord Ratio Wings With Lateral Jets," AD-733858, FTD-HC 23-319-71, Oct., 1971.

20. Briggs, M. M., and R. G. Schwind, "Augmentation of Fighter Aircraft Lift and STOL Capability by Blowing Outboard from the Wing Tips," AIAA paper No. 83-0078, AIAA 21st Aerospace Sciences Meeting, Reno, Nevada, January, 1983.

21. Yuan, S. W., and Bloom, A. M., "Experimental Investigation of

Wing-Tip Vortex Abatement," Proceedings of the 9th Congress of the International Council of the Aeronautical Sciences, Ed. R. R. Exter and J. Singer, Haifa, Israel, August, 1974.

22. Crow, S. C., "Stability Theory or a Pair of Trailing Vortices," AIAA Journal, Vol. 8, pp. 2172-2179, December ,1970.

23. Jones, W. P. and Chevalier, H. L., "Aircraft Trailing Vortex Instabilities," Proceedings of the 9th Congress of the International Council of the Aeronautical Sciences, edited by R. R. Exter and J. Singer, Haifa, Israel, pp. 293-302, August, 1974.

24. Fearn, R. L. and Weston, R. P.,"Vorticity Associated with a Jet in a Cross Flow," AIAA Journal, Vol. pp. 1666-1671, December, 1974.

25. Chen, Z. L. and Wu, J. M., "Jet Wing Vortex Lattice Theory With Nonlinear Wake and Tip Flows," AIAA Paper No. 83-0263, 21st Aerospace Sciences Meeting, Reno, Nevada, Jan. 1983.

26. Abramovich, G. N., "The Theory of Turbulent Jets," The M.I.T. Press, Cambridge, Mass., 1963.

27. Keffer, J. F., "The Physical Nature of the Subsonic Jet in a Cross-Stream," NASA SP-218, pp. 19-37, 1969.

28. McMahon, H. M., and Mosher, D. K., "Experimental Investigation of Pressures Induced on a Flate Plate by a Jet Issuing into a Subsonic Crosswind," NASA SP-218, pp. 49-62, 1969.

29. Sucec, J. and Bowley, W. W., "Prediction of the Trajectory of a Turbulent Jet Injected into a Crossflowing Stream," J. of Fluid Eng., pp. 667-673, Dec. 1976.

30. Monical, R. E., "A Method of Representing Fan-Wing Combination for 3-D Potential Solution," J. of Aircraft, Vol. 2, No. 6, pp. 527-530, 1965.

31. Margason, R. J., "The Path of a Jet Directed at Large Angles to a Subsonic Free Stream," NASA TN D-4919, 1968.

32. Gilliam, F. T., "An Investigation of the Effects of Discrete Wing Tip Jets on Wake Vortex Roll Up," Ph.D. Dissertation, The University of Tennessee Space Institute, Aug. 1983.

33. Chow, Chuen-Yen, Computational Fluid Mechanics, New York: John Wiley and Sons, 1979.

34. Moore, D. W., "A Numerical Study of the Roll-Up of a Finite Vortex Sheet," Journal of Fluid Mechanics, 63 (Part 2): 225-235, 1974.

35. Clements, R. R. and Maul, D. J., "The Rolling Up of a Trailing Vortex Sheet," Aeronautical Journal, pp. 45-51, 1973.

36. Keffer, J. F., and Baines, W. D., "The Round Turbulent Jet in a Cross-Wind," J. of Fluid Mechanics, Vol. 15, pp. 431-447, 1963.

37. Kamotani, Y. and Greber, I., "Experiments on a Turbulent Jet in

a Cross Flow," AIAA Journal, Vol. 10, pp. 1425-1429, November, 1972.

38. Krausche, D., Fearn, R. L. and Weston, R. P., "Round Jet in a Cross Flow: Influence of Injection Angle on Vortex Properties," AIAA Journal, Vol. 16, pp. 636-637, June, 1978.

*U.S.Government Printing Office: 1984 - 559-065/20568

END

FILMED

2-85

DTIC